Growth of CdTe/CdZnTe Single Crystals by the Vertical Gradient Freezing Method

by

Lingzhi Li
B.Sc., Harbin University of Science and Technology, 1983
M.Sc., Harbin Institute of Technology, 1988

A Thesis Submitted in Partial Fulfillment of the
Requirements for the Degree of

MASTER OF APPLIED SCIENCE

in the Department of Mechanical Engineering

We accept this report as conforming
to the required standard

[redacted]

Dr. S. Dost, Supervisor (Department of Mechanical Engineering)

[redacted]

Dr. Y. Stepanenko, Co-Supervisor (Department of Mechanical Engineering)

[redacted]

Dr. M. Whale, Department Member (Department of Mechanical Engineering)

[redacted]

Dr. H. H. L. Kwok, Outside Member (Department of Electrical and Computer Engineering)

[redacted]

Dr. J. Bornemann, External Examiner (Department of Electrical and Computer Engineering)

University of Victoria

Supervisors: Dr. Sadik Dost and Dr. Yury Stepanenko

ABSTRACT

Single crystals of CdTe/CdZnTe are important semiconducting materials for the development of x-ray and γ-ray detectors. They can also be used as substrates for the epitaxial growth of HgCdTe, which is a key material for far-infrared detectors with high resolution and large detection area. Currently, there are no mature techniques to grow CdTe/CdZnTe single crystals, and the cost of these materials for commercial purposes is still high. In this thesis, a combined experimental/theoretical study is undertaken. The phenomena of supercooling and superheating of CdTe/CdZnTe, which play an important role in the quality and size of grown crystals, are discussed. A VGF crystal growth facility and a growth procedure for CdTe/CdZnTe are developed. A unique technique (temperature profile) is designed to take advantages of superheating and confine the detrimental effect of supercooling during crystal growth. The electrical properties and defect structures of the CdTe/CdZnTe crystals grown by this VGF facility are also analyzed and reported.

Examiners:

[redacted]

Dr. S. Dost, Supervisor (Department of Mechanical Engineering)

[redacted]

Dr. Y. Stepanenko, Co-Supervisor (Department of Mechanical Engineering)

[redacted]

Dr. M. Whale, Department Member (Department of Mechanical Engineering)

[redacted]

Dr. H. H. L. Kwok, Outside Member (Department of Electrical and Computer Engineering)

[redacted]

Dr. J. Bornemann, External Examiner (Department of Electrical and Computer Engineering)

Table of Contents

List of Tables

List of Figures

Glossary of Acronyms

Acronym	**Definition**
BN	Boron Nitride
CRSS	Critical Resolved Shear Stress
FWHM	Full Width at Half Maximum
HB	Horizontal Bridgman
HPBM	High Pressure Bridgman Method
HPVB	High Pressure Vertical Bridgman
LEC	Liquid Encapsulated Czochralski
PBN	Pyrolytic Boron Nitride
PVTM	Physical Vapor Transport Method
6N	6 Nines
TC	Thermocouple
THM	Travelling Heat Method
VGF	Vertical Gradient Freezing
VB	Vertical Bridgman

Acknowledgments

I would like to thank my supervisors, professors Dr. Sadik Dost and Dr. Yury Stepanenko, for their constant assistance and guidance throughout my program. I would also like to thank them and the Amistar Research and Development Inc. for their financial support.

I am grateful to Nick Audet for his help on experimental apparatus and encouragement throughout the project. I am also grateful to Dr. Yasunori Okano for his useful information and literatures.

Many thanks to Rodney Katz for his help on the designing and machining the crystal growth facilities and John R. Butler for crystal processing.

Chapter 1 Introduction

1.1 Background

Detection of x-ray and γ-ray radiation is done best by solid-state detectors because of their low ionization energy, high energy resolution, high sensitivity, and compactness and convenience. Since such detectors use single crystal semiconducting materials, the research on semiconductor materials for such detectors has been very intensive in the past 30 years. The most common commercially available materials for such detectors are Si and Ge, which have been used for years successfully. However, there are problems inherent in these materials, such as high thermal noise and low absorption. For reliable detection, these problems must be overcome. This goal can only be achieved by finding new single crystal semiconducting materials that will not have such problems. A class of such new materials is Cadmium Telluride (CdTe) and Cadmium Zinc Telluride (CdZnTe) single crystal II-VI semiconducting compounds.

CdTe/CdZnTe crystals have mainly three physical properties that exhibit advantages over Ge and Si crystals. These physical properties are high atomic number (48-52), wide energy band gap (1.47eV), high resistivity (over 10^8 $\Omega\cdot$cm) at room temperature, and also good charge-carrier mobilities (over 1000 $cm^2/V.Sec.$ for electrons and 100 $cm^2/(V.Sec.)$ for holes, here V is volt). These properties of some materials are listed in Table 1 for comparison purpose (Fraden, 1993). The research on HgI_2 is still in its early investigating stage (Schieber, 1989). Below we discuss the significance of these physical properties.

Table 1. Properties of Some Semiconductors.

Material (operating temperature in K)	Atomic number Z	Band Gap EV	Energy per electron-hole pair, eV
Si (300)	14	1.12	3.61
Ge (77)	32	0.74	2.98
CdTe (300)	48-52	1.47	4.43
HgI_2 (300)	80-53	2.13	6.5

Atomic number: The atomic number is one of the important parameters in selecting the best materials for detection purpose. The photoelectric interaction is stronger in materials of high atomic number. The probability of the photoelectric interaction occurring is roughly proportional to Z^n, where n is between 4 and 5 and Z is the atomic number (see appendix 1). Since the atomic number of CdTe is much higher than that of Si and Ge, it is expected that CdTe/CdZnTe crystals would be more efficient for detecting x-rays and γ-rays.

Energy band gap: The energy band gap of Ge is not large; therefore the detectors based on this material must be stored and operated at low temperatures (liquid-nitrogen temperature). The maintenance and operation of such devices are therefore expensive and inconvenient. The larger band gap of CdTe/CdZnTe, on the other hand, permits these detectors to be operated and maintained at room temperature. In addition, the associated thermal effect (thermally generated leakage current) may be negligible. This very important property of CdTe/CdZnTe crystals provides a significant advantage over other competing materials.

High resistivity: The high resistivity is another property of CdTe/CdZnTe crystals that provides another advantage over other materials. The resistivity can be controlled to over 10^{10} Ω·cm. Such a high resistivity makes detector structures simple and leakage current low. For instance, due to its low resistivity, Si detectors need a special structure to block the leakage current, because the current is 3-5 orders of magnitude greater than a radiation-induced electric current.

Based on these three physical properties alone, as discussed above, it is evident that CdTe and $Cd_{1-x}Zn_xTe$ crystals are excellent candidates for x-ray and γ-rays detectors operating at room temperature.

Carrier mobility: The mobility of a carrier is an important characteristic of semiconductors. Devices based on semiconductors of higher mobility will be faster. Since the carrier mobility of CdTe/CdZnTe crystals is high, the x-ray or γ-detectors based on CdTe/CdZnTe crystals will respond faster.

Substrates lattice matched to infrared materials In addition, CdTe/CdZnTe single crystals have an important feature that is useful in the development of infrared detectors. They can be used as substrates for the epitaxial growth of $Hg_{1-y}Cd_yTe$ which is a key material (and also a key technology) for far-infrared detectors with high resolution and large detection area. For $Cd_{1-x}Zn_xTe$, when x is equal to 0.03~0.04, the lattice constant is close to that of $Hg_{0.8}Cd_{0.2}Te$ whose energy gap corresponds to a 10 μm wavelength. This leads to a better lattice match and also less dislocation generated at the substrate/epilayer interface. The alloying of ZnTe into CdTe also improves crystalline hardness, increases the critical resolved shear stress (CRSS) and band gap (Qadri, 1985). CdZnTe should exhibit higher quality than CdTe.

The physical parameters discussed above and also the requirements of radiation detectors suggest that CdTe/CdZnTe semiconducting crystals with certain characteristics (such as large diameter, defect densities below 10^5 per cm^2, high resistivity and good physical uniformity) can meet the demand of the x-ray and γ-ray detectors industry. However, such materials presently are not available. If these materials can be grown reproducibly, x-ray and γ-ray detectors with better characteristics can be developed. The objective of this thesis is to develop a reproducible means of obtaining such materials.

There have been numerous attempts to grow CdTe/ $Cd_{1-x}Zn_xTe$ single crystals using a variety of growth techniques. The first large diameter crystal (75 mm diameter × 40 mm length) was grown by Oda et al. in 1986 (O.Oda, 1986) by the vertical gradient freezing method (VGF). Later, Azoulay et al. (M.Azoulay, 1990), using the seeded VGF method, grew 50 mm diameter × 40 mm length crystal in 1990. Until now, the largest twin-free CdZnTe crystal (100 mm in diameter) reported was grown by Asahi et al. (T.Asahi, 1996) using the VGF method. In their experiment, they used a multiple-zone furnace to control the temperature profile. Butler et al. (J. F. Butler, 1993) grew 100 mm diameter ingots using the high pressure vertical Bridgman method (HPVB). Also, Grasza et al. (K. Grasza, 1992) and Palosz (W. Palosz, 1995) used the physical vapor transport method to grow high quality crystals. Chibani et al. (L. Chibani, 1996) grew detector-grade CdTe:Cl and CdZnTe crystals by the travelling heater method (THM) and the high pressure Bridgman method (HPBM), respectively.

In spite of these attempts and progress made in this area, numerous problems still remain. Up to now, it has not been possible to grow single crystals of CdTe/CdZnTe from the melt in a reproducible manner. The grown crystal boules are usually characterized by the presence of grain boundaries, twin lamellas, cracks and certain dislocation density. The difficulties encountered in growth of CdTe/CdZnTe crystals are due to the following physical properties (T. Asahi, 1995) of CdTe/CdZnTe:

(1) *Low thermal conductivity*: Since the heat released during solidification cannot be dissipated because of low thermal conductivity, it becomes difficult to control the melt/solid interface shape as desired.

(2) *The low stacking fault energy*: Twinning takes place easily due to the temperature fluctuation during crystal growth due to low fault stacking energy.

(3) *The low critical resolved shear stress:* dislocations are easily generated due to the stress from the container and the thermal stress during crystal growth due to low critical resolved shear stress.

The deformation of defect structures of II-VI group crystal compounds is very sensitive to growth conditions. Much effort is required to optimize the growth conditions such as the technique for preparing source materials, pressure within the growth furnace, growth rate of crystals, cooling rate, and post-growth heat treatments.

Another difficulty that requires attention in growing CdZnTe crystals is the non-uniformity of Zn content in the crystal. The segregation coefficient of Zn in CdTe is 1.16-1.35 (T. S. Lee, 1995), which gives rise to a non-uniform Zn distribution in both axial and radial directions, severely reducing yields of useful material.

All the existing techniques developed so far for the growth of CdTe/CdZnTe crystals are still far from being mature. Great efforts are necessary to improve these techniques for the growth of reproducible crystals with higher quality and lower cost.

1.2 Growth techniques

For commercial growth of III-V semiconductors compounds and alloys, the Bridgman (including both horizontal (HB) and vertical (VB)), the Vertical Gradient Freezing, and the Liquid Encapsulated Czochralski (LEC) are the most conventional and commonly used growth techniques.

Although the LEC is one of the most commonly used commercial growth techniques, it is not appropriate for the growth of CdTe/CdZnTe crystals. In LEC, the charge is held in a crucible and then heated until it melts. The melted charge material, called "the melt", is covered deliberately with a liquid coating and kept under pressure with a pressurized inert gas. This is needed to prevent the loss of melt material due to the high vapour pressure of melt materials. By placing a seed crystal in contact with the melt, the growth is then achieved by slowly withdrawing the seed from the melt. During growth, the seed is rotated relative to the melt to promote a better mixing and a uniform temperature distribution. Cd and Zn single elements have very high vapour pressures at high temperatures. Cd vapor pressure is as high as 13 atms at the melting point of CdTe, and that of Zn is about 10 atms at the melting point of ZnTe (V. M. Glazov, 1969). In order to prevent the loss of melting material in LEC growth, the pressure in the crucible must be kept higher than the highest vapour pressure. This is very difficult to achieve by a pressurized inert gas. In addition, the thermal conductivity of CdZnTe is smaller than that of the B_2O_3 encapsulant, which makes it very difficult to grow large CdTe/CdZnTe crystals from their seed crystals.

In VB (HB), a seed is placed in contact with the melt (or without seed), and the melt is solidified unidirectionally. The growth can be achieved in these techniques by one of the following two ways: either by moving the melt relative to a stationary temperature gradient or by moving the furnace relative to the melt. In VGF, both the crucible and the furnace are stationary and only the temperature profile is changed. In other words, a linear temperature gradient is maintained in a certain area, and then, starting from the tip, is moved towards the low temperature region progressively, forcing the freezing isotherm to move up along the crucible. VB (L. G. Casagrande, 1994; J. Shen, 1993; F. P. Doty, 1992), HB (P. Brunet, 1993) and VGF (T. Asahi, 1996) are the most suitable methods for the growth of predominantly single crystalline semiconductors of CdTe/CdZnTe.

There are also other methods to grow $Cd_{1-x}Zn_xTe$ single crystals, such as the Traveling Heater Method (THM) (R. Triboulet, 1981; R. U. Barz, 1997) and the Physical Vapor Transport Method (PVTM) (W. Palosz, 1995). Both methods can grow high quality II-VI semiconductors.

THM is a solution growth technique and appropriate for producing high resistivity and high purity CdTe/CdZnTe single crystals. THM has the advantage of being able to grow high purity materials. This is because, being a solution technique, impurities can be removed during growth. However, THM suffers from extremely low growth rate limits due to the low solute concentration in the solution and the slow mass transport from the dissolving solid to the growth interface. Although the solution growth techniques such as THM and LPEE (S. Dost, 1995 and 1996) can grow very thick crystals, the solution growth is generally not considered as a bulk growth technique.

The physical vapor transport method is a promising method to grow high purity single crystals. The high vapour pressures of II-VI compounds allow the growth of materials similar to CdTe/CdZnTe from the vapour at temperatures below their congruent melting points. However, the growth rate is also low and growth time correspondingly long. In the following, some of the methods particularly useful to CdTe/CdZnTe growth are described in detail.

1.2.1 Bridgman techniques

Both the horizontal and vertical Bridgman techniques grow bulk crystals from the melt. Typical sketches of vertical and horizontal Bridgman furnaces are shown in Figure 1 and Figure 2.

In the horizontal Bridgman, the single element materials are contained in a boat. The seed is fixed at one side of the boat. The thermal environment of the boat consists of three zones: a hot zone, an insulating section, and a cold zone. During growth, the boat is slowly moved to the left after the materials are melted in the crucible. When the seed passes through the temperature gradient between the cold and the hot zones, the liquid solidifies on the seed and forms single crystal solid. The boat moves until all the liquid becomes solid crystal.

In the vertical Bridgman, the melt material is contained in a cylindrical ampoule at the bottom of which the solidification starts from a crystal seed (or without a seed). The thermal environment of the ampoule is the same as that of the horizontal setup, and also consists of three zones: hot, insulating, and cold. During growth, the ampoule is slowly moved downwards. In other words, the temperature profile induced by the environment in the solid and the melt moves

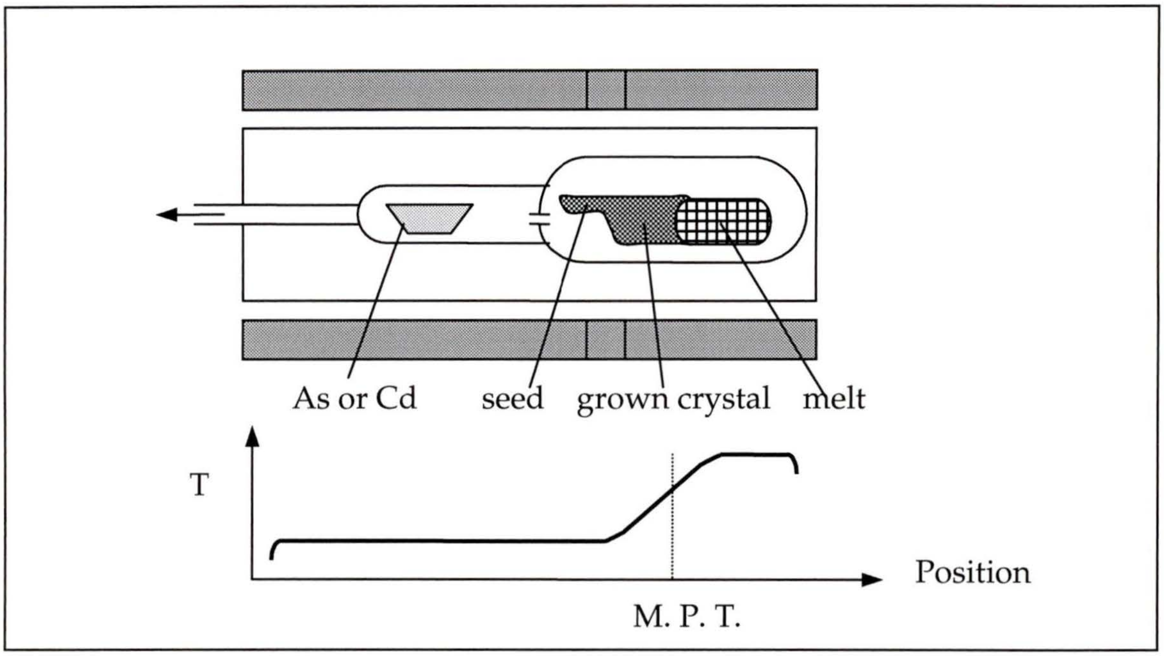

Figure 1. Schematic diagram of a HB furnace.

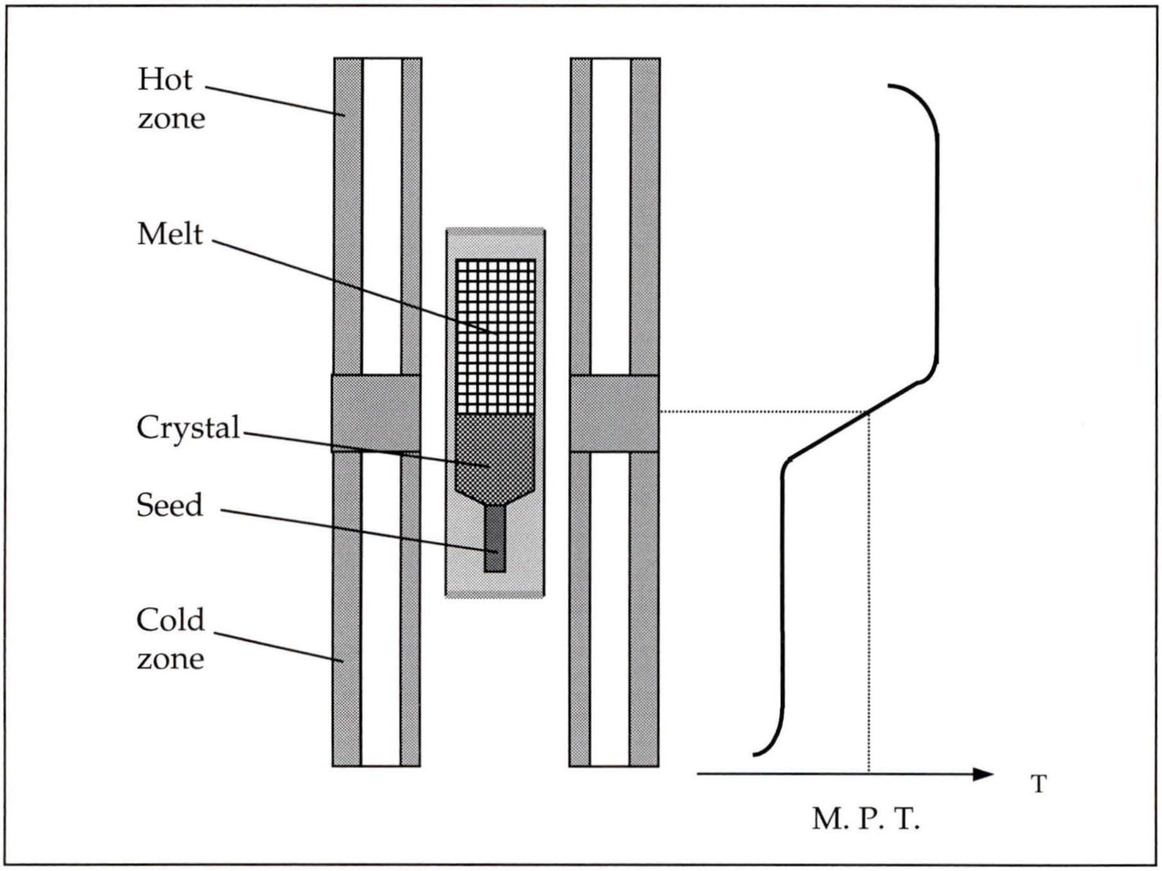

Figure 2. Schematic diagram of a VB furnace.

upward relative to the ampoule. During the process the axial temperature profile is kept unchanged. Melt solidifies progressively until the crystal is completely formed. A major advantage of the vertical Bridgman technique over the horizontal one is that the solid phase is located under the liquid phase and that the temperature gradient is pointing essentially upwards in the melt. Other advantages of the vertical method are (E. Monberg, 1994): (1) The crucible and the furnace can be designed with an axisymmetry, resulting in axisymmetric convective fluid flow, temperature and concentration fields. This leads to the growth of more homogeneous crystals. (2) In commercial crystal growth, the vertical setup has a distinct economic advantage. Since the grown crystals have a circular symmetry, circular wafers can be obtained. On the other hand, the boules grown by the horizontal Bridgman yields D-shaped wafers. But both the horizontal and vertical setups have a common major disadvantage that the temperature distribution in the furnace changes in time due to the movement of the melt (a material with a large heat-capacity) during growth, affecting the quality of grown crystals as well as the growth conditions. The situation becomes worse when more melt material is used to grow larger crystals. Mechanical movement of the heater or ampoule may also induce undesired vibrations during the growth.

1.2.2 The VGF technique

In the vertical gradient freezing method (VGF), the temperature gradient can be controlled very effectively. The furnace consists of several thermal zones monitored by relative thermocouples. It is not necessary to move either the ampoule or the furnace. The selected temperature profile is moved upwards by only controlling the temperatures of the zones of the furnace. In VGF growth, in addition to the above-mentioned advantages of the vertical Bridgman method, there are no moving mechanical parts and no induced vibrations. The structure of VGF is almost the same as that of the VB, except that both the melt and the heater are stationary. Figure 3 shows schematics of a VGF furnace.

1.2.3 The THM technique

In both the Bridgman and the VGF methods, the feed materials are charged roughly in stoichiometry because it could not be maintained in strict stoichiometry theoretically. In THM, however, the crystal stoichiometry is not maintained in the liquid phase. The typical THM setup consists of a solution contained between two layers of crystals; the charge material being on top, and the seed on the bottom. Growth is initiated and sustained by passing the crucible through a temperature profile controlled by the heater. The temperature is typically about 100°C lower than the melting point of the compound. The configuration of THM is shown in Figure 4. The charge material is polycrystalline. The solvent is a solution of tellurium and cadmium. Seeding is accomplished by using oriented CdTe/CdZnTe single crystal. The typical growth rate is about 1~2mm/day.

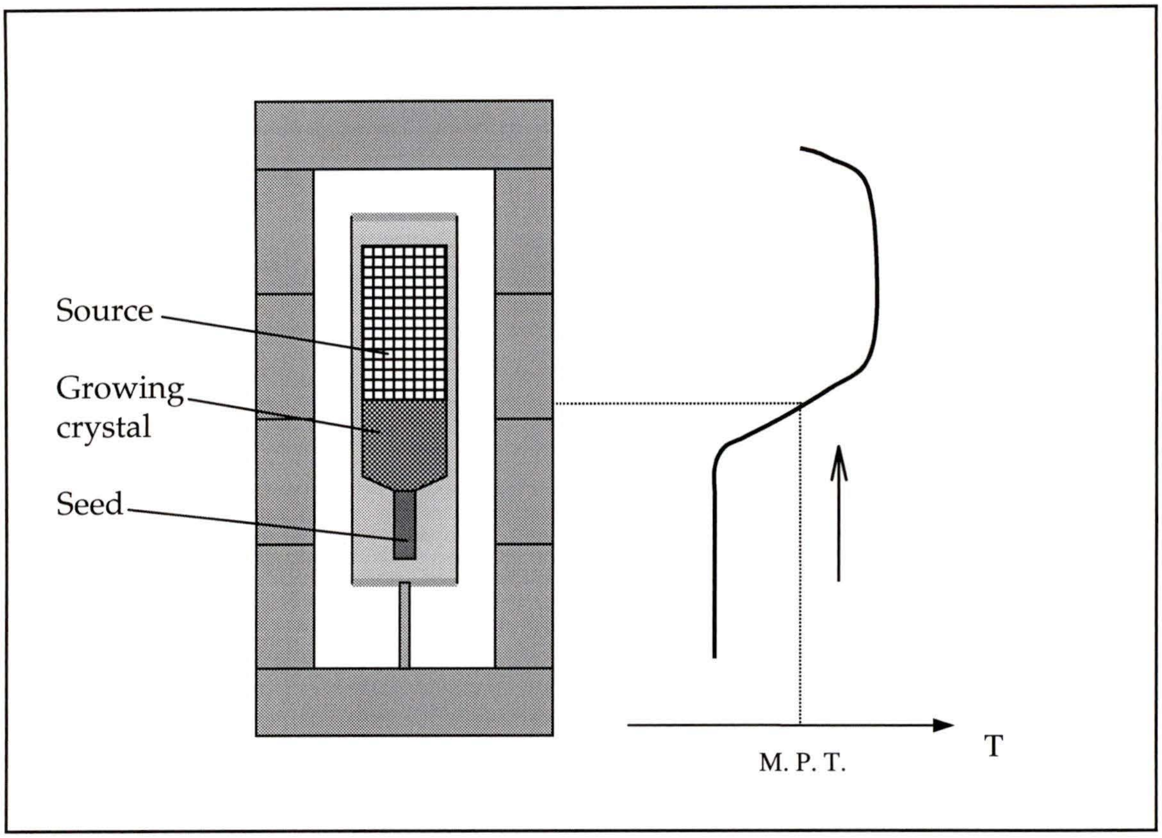

Figure 3. Schematic diagram of a VGF furnace.

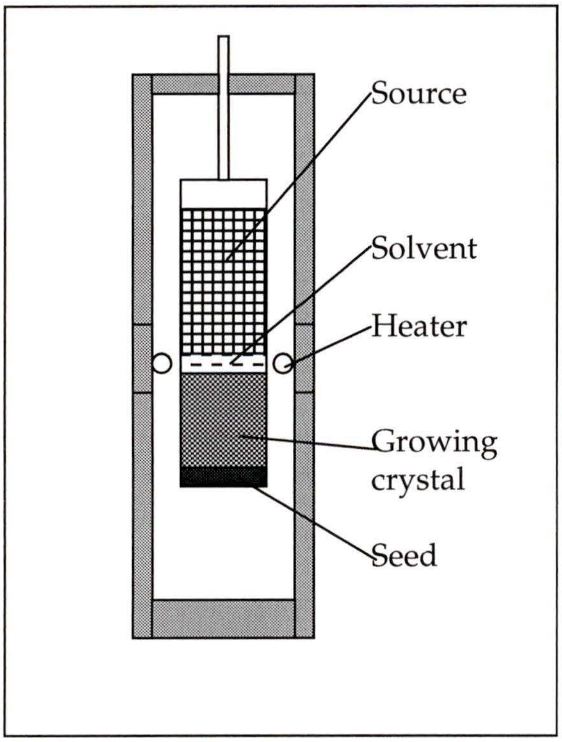

Figure 4. THM furnace diagram.

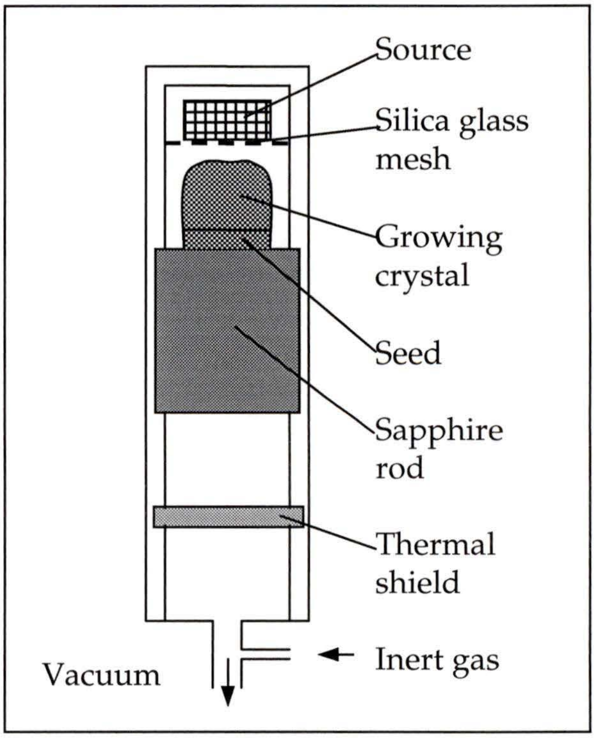

Figure 5. PVT growth diagram.

1.2.4 The PVT technique

The vapor growth technique has several advantages. The grown crystals have less point defects and low dislocation densities due to the nature of the technique, and the growth is achieved at relatively low temperatures compared with the melting temperatures. There are several kinds of vapor growth techniques such as unseed and seed vapor growth, and the sublimation travelling heater method. Figure 5 (E. Kaldis, 1994) shows a typical schematic of a PVT setup. Crystals are grown on a sapphire rod with a diameter of up to 10 cm. The source material lying on a quartz grid above the seed is transported through a rather close space to the growing crystal.

CdTe/CdZnTe semiconductors grown by THM and PVT are of high quality and low defect density, but the low growth rates limit their production. Today, most commercially available CdTe/CdZnTe wafers are still grown by either the vertical (horizontal) Bridgman techniques or by the vertical gradient freezing technique.

Both the Bridgman and the VGF methods belong to the melt growth category. In the melt growth the driving force for solidification is the movement of an imposed normal temperature gradient relative to the liquid-solid interface. The factors controlling the growth process are the steepness of temperature gradient and the relative movement rate between the temperature gradient and the interface. If the selected temperature gradient is too small, supercooling will break down the planar liquid-solid interface leading to a cellular or dendritic structure. If the temperature gradient is too high, severe lattice strains on the solidified material will cause dislocation generation or cracking. To achieve, at the same time, a desirable growth rate and also a stable interface, the control of the temperature gradient is especially crucial in the growth CdTe/CdZnTe crystals.

Being a solution growth, the driving force for crystallization in THM is the super-saturation in the liquid. The concentration gradient is established in the solution above the growth surface. The absorbed atoms can be accommodated at the correct lattice sites on the growth surface.

1.3 Composition control in melt growth

It is found (P. Rudolph, 1993) that compositions of CdTe/CdZnTe compounds affect their electrical and optical properties to a large extent. Also, if conventional vertical ampoules are filled with stoichiometrically adjusted starting material and there is an "empty space" with no material above the charge material, the crystal growth process will always begin from a tellurium-rich melt. Inclusions and precipitates of crystal imperfection will arise by the solidification from tellurium-rich melts. Therefore, growth from stoichiometry is one of the most important aspects in crystal growth.

Different techniques were developed by various researchers to control the melt compositions. The first method was to use an inert gas to overcome the cadmium pressure. F. P. Doty and J. F. Butler use the high-pressure Bridgman method to grow CdZnTe (F. P. Doty, 1992). In this method, an inert gas over pressure reduces the mean free path for vapour species, reducing diffusion. The use of high pressure inhibits evaporation of the charge and reduces loss of material from the melt. N. N. Kolesnikov et al. also used the vertical high-pressure Bridgman technique (N. N. Kolesnikov, 1997). They employed a two-step growth process. In the first step, the starting ZnTe-CdTe mixtures were compacted into polycrystalline ingots under 5 MPa argon pressure. In the second step, CdZnTe crystals were grown with different Ar pressures (2, 4, 5 and 8 MPa). They found that the applied Ar pressure did affect the CdZnTe composition uniformity, and that the increase of x in $Cd_{1-x}Zn_xTe$ required the increase of the Ar pressure in order to achieve a uniform composition. Resistivities over 10^9 Ω·cm were obtained in some of the samples they used. Etch pit densities are at the range of 7×10^3-5×10^4 cm^{-2} when zinc composition is 0.2.

In another method used by P. Rudolph to control the melt composition, an additional Cd excess is scaled to produce a near stoichiometric molten starting charge which compensates for loss of Cd evaporation into the empty space in the ampoule (P. Rudolph, 1993). It roughly requires the use of about 2-3 · 10^{-3}% excess Cd to give a sufficient overpressure of Cd to grow crystals with a nearly stoichiometric composition. The amount of excess Cd also depends on the volume of empty space above the material.

In the third method to control the melt composition, a Cd reservoir is used during growth. This excess Cd reservoir is separated from the charge material but connected to the empty space in the ampoule. T. Asahi et al used this technique to grow a 100-mm in diameter twin-free single crystal (T. Asahi, 1996). The temperature of the Cd reservoir was controlled at 785 °C. Grown $Cd_{0.97}Zn_{0.03}Te$ single crystals were of p-type conductivity. Resistivities, carrier concentrations and Hall mobilities were respectively 30-37 Ω·cm, $(2.1\text{-}2.2) \times 10^{15}$ cm^{-3}, and 80-100 cm^2 V^{-1} s^{-1}. Etch pit densities are at the range of $(4\text{-}6) \times 10^4$ cm^{-2}. Cheuvart et al (P. Cheuvart, 1990) also used the Cd source method and obtained resistivities over 10^7 Ω·cm. Rudolph et al (P. Rudolph, 1993) showed that crystals grown by the Cd source technique are usually characterized by very low hole concentrations $10^{11} - 10^{13}$ cm^{-3}, which are nearly homogeneously distributed along the growth direction.

Among these three methods, the one with a Cd reservoir is the most widely used technique. The use of a source of Cd vapour pressure provides more freedom to control the composition of the melt. In the process of synthesis, the risk of explosion is reduced when a quartz tube is used as a crucible, because the Cd reservoir can be set at a constant vapour pressure or temperature during the entire growth process. During growth, melt uniformity is enhanced by the thermal convection - the convective flow in the melt due to temperature gradients. The Cd source technique is also convenient for controlling the resistivities of CdTe/CdZnTe crystals, by simply changing the growth conditions with different Cd vapour pressures. In addition, it is also possible to program the control during the post growth annealing of the whole crystal.

1.4 Application for x-ray detectors

As mentioned at the beginning of this chapter, one of the important applications of CdTe/CdZnTe semiconducting single crystals is their use as x-ray (γ-ray) detector materials. CdTe/CdZnTe radiation detectors have advantages of a large absorption coefficient, compact size, simple assembly and room temperature operation compared with other type detectors. Currently used x-ray (γ-ray) detectors are high purity Ge detectors and Si detectors. Ge detectors only operate at the liquid-nitrogen temperature. Maintaining the cooling system is expensive and inconvenient for many applications such as nuclear verification and medical imaging. Si detectors are not efficient enough to detect γ-rays.

In recent years, a large body of research has been conducted on practical applications of CdTe/CdZnTe crystals in various fields such as radiation detecting (M. Ohmori, 1993; J. F. Butler, 1993; L. Chibani, 1996), medical diagnostics and dosimetry (G. Entine, 1989). These studies have demonstrated the potential of CdTe/CdZnTe crystals for applications in nuclear verification and safe guard, medical imaging, and x-ray (γ-ray) astronomy. Butler et al grew CdZnTe crystals by a high pressure Bridgman method (HPB). A detector made from HPB-grown CdTe crystals was maintained under a constant bias of 50V over three years on-line in an industrial environment. There was no measurable change in its counting efficiency during this period. They also presented an energy spectrum of the γ-ray emission from an Am-241 source using a $Cd_{0.8}Zn_{0.2}Te$ detector (Figure 6). The detector was biased at 300 V, and its dimensions were 5 mm × 5mm × 1.2 mm. The linewidth or the full width at half maximum (FWHM) of the 59.5 keV photopeak is less than 6% (3.6 keV). M. Ohmori and Y. Iwase, on the other hand, used CdTe crystals grown by THM to fabricate single-element detectors, array detectors and monolithic detectors. Figure 7 shows the energy spectrum of one-element detector with an Am-241 source. The detector was biased at 24 V and its dimensions were 1.8 mm × 2.0 mm × 1.2 mm. The linewidth of the 60 keV photopeak is 4.0 keV. For array detectors, the dimensions of each element are 1.8 mm × 2.0 mm × 1.2 mm. The element pitch is 2.0 mm and the total detective length is 180 mm. The monolithic detector consists of with 20 detecting elements, each of which has a width of 0.35

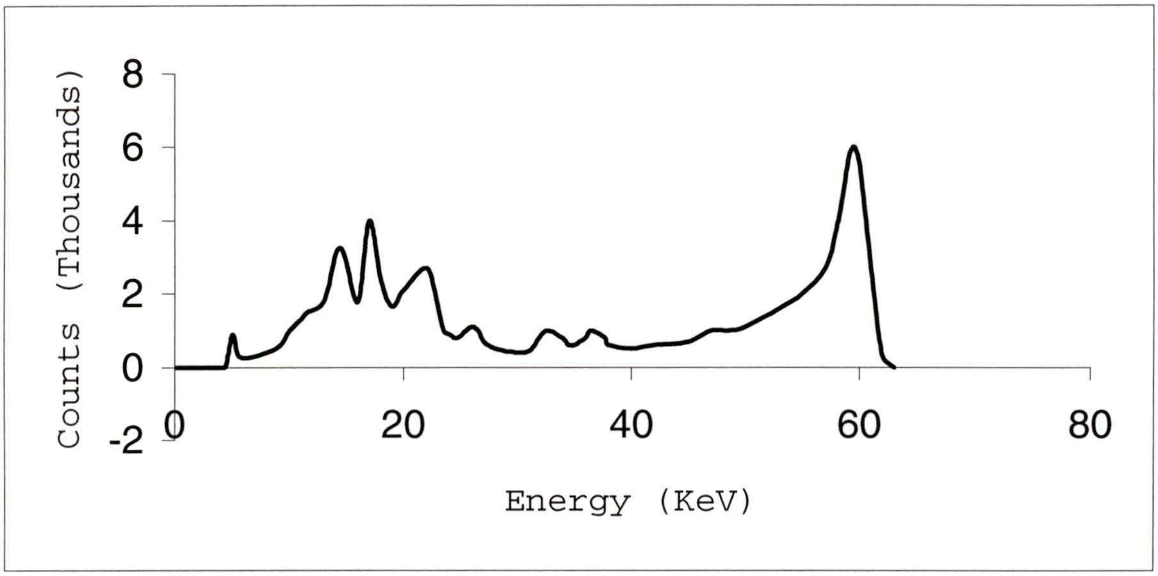

Figure 6. Energy spectrum measured with a $Cd_{0.8}Zn_{0.2}Te$ detector.

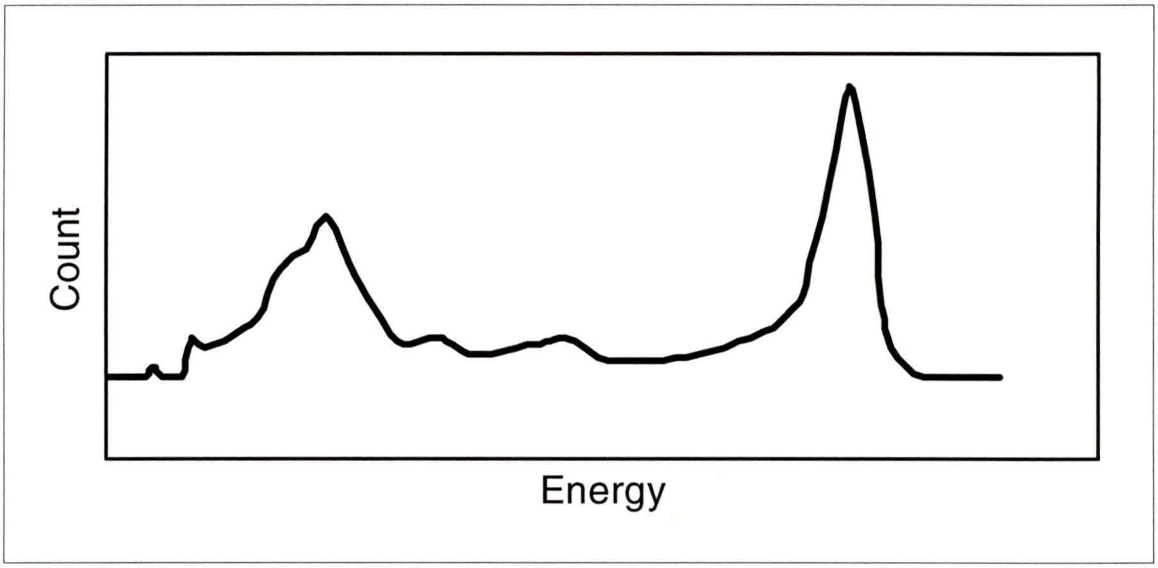

Figure 7. Measured energy spectrum for a 60 keV γ-ray source.

mm, a length of 10 mm, a thickness of 1.2 mm and a pitch of 0.5 mm. The averaged FWHM and count rate were 8.9 keV and 1.6 kcps. The mean lifetime is estimated to be 109 h at 25°C.

1.5 Purpose and outline

This work was motivated by the need for growing homogeneous, crack-free CdTe/CdZnTe semiconductor crystals suitable for x – ray detectors. This thesis reports the results of an experimental study conducted on the melt growth of CdTe/CdZnTe crystals by the VGF method. Some problems existing in the growth of CdTe/CdZnTe crystals, which are critical in growth of all II – VI crystals, such as supercooling and thermal stresses during crystal growth are discussed, and measurements of electrical and structural properties of the grown crystals are presented.

In Chapter 1, a short introduction including the historical developments in crystal growth, features of various growth techniques and the related literature to date is presented. In Chapter 2 the related theory of crystalline structures is briefly introduced. A summary of CdTe/CdZnTe crystal properties is given in Chapter 3. In Chapter 4, the experimental facility is introduced and the crystal growth procedure and growth conditions are presented in detail. At the end of this chapter, the grown ingots are analyzed. In Chapter 5, the electrical and structural characteristics of grown crystals are given, and the results are discussed. Concluding remarks are presented in Chapter 6.

Chapter 2 Fundamentals of Crystalline

2.1 Crystal structures

All atoms in a crystal occupy positions (points) which are located in certain geometrical patterns. These geometrical patterns are usually described by two kinds of lattice representations: the Bravais lattice or non-Bravais lattice. In a Bravais lattice, all lattice points are equivalent, in other words, all the atoms located at the lattice points are the same kind. In a non-Bravais lattice, some of the lattice points are nonequivalent. The non-Bravais lattice may be regarded as a combination of two or more interpenetrating Bravais lattices with fixed orientations relative to each other.

There are 14 different Bravais lattices. They are listed in Table 2. The symbols $\mathbf{a}$, $\mathbf{b}$, and $\mathbf{c}$ represent the base vectors, and α, β and γ, respectively, stand for the angles between base vectors. They are indicated in Figure 8 for a cubic crystal. Simple cubic and face-centered cubic structures are shown in Figure 9.

Most crystalline semiconductors belong to the cubic structure system. C, Ge, and Si belong to the diamond structure, the unit cell of which is a face-centered cubic cell. Its basis is made of two atoms and each atom finds itself surrounded by four nearest atoms (see Figure 13), which form a regular tetrahedron. Such a structure is commonly found in semiconductors and is referred to as a tetrahedral bond. The structure of Zinc sulfide (ZnS) is closely related to the diamond structure. The only difference is that the two atoms forming the basis are of different kinds (Zn and S). Many of the crystal semiconductors belong to this kind of structure, such as InSb, GaSb, GaAs and CdTe. This kind of structure is known as the zincblende structure.

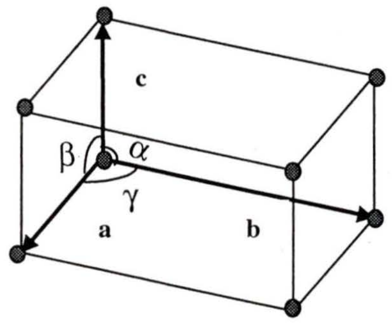

Figure 8. Unit cell specified by the base vectors and angles.

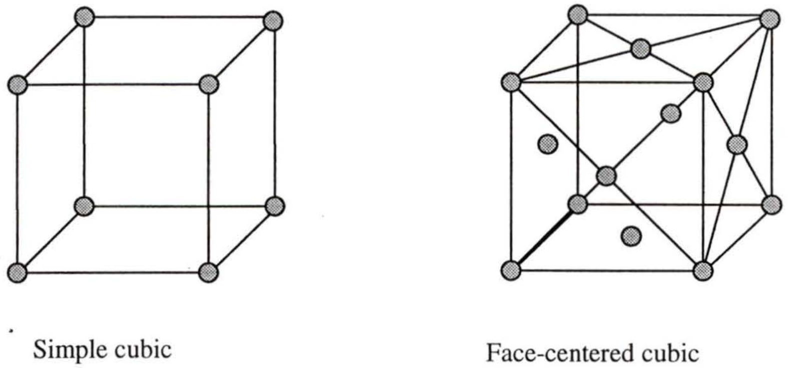

Figure 9. Simple cubic and face-centered cubic structures.

Table 2. Fourteen Bravais lattices.

System	Bravais lattice	Unit cell characteristic
Triclinic	Simple	$a \neq b \neq c$ $\alpha \neq \beta \neq \gamma \neq 90^\circ$
Monoclinic	Simple Base-centered	$a \neq b \neq c$ $\alpha = \beta = 90^\circ \neq \gamma$
Orthorhombic	Simple Base-centered Body-centered Face-centered	$a \neq b \neq c$ $\alpha = \beta = \gamma = 90^\circ$
Tetragonal	Simple Body-centered	$a = b \neq c$ $\alpha = \beta = \gamma = 90^\circ$
Cubic	Simple Body-centered Face-centered	$a = b = c$ $\alpha = \beta = \gamma = 90^\circ$
Trigonal	Simple	$a = b = c$ $\alpha = \beta = \gamma \neq 90^\circ$
Hexagonal	Simple	$a = b \neq c$ $\alpha = \beta = 90^\circ$ $\gamma = 120^\circ$

2.2 Miller indices in cubic system with orthogonal axes

The orientation of a plane in a lattice is specified by its Miller indices, which are defined as follows (H.W. King, 1997):

- Set the crystal with its base vectors parallel to the orthogonal axes and mark off the length on axes in the unit cell of the crystal.
- Count the number of intercepts which the plane makes on the three axes.
- Take the reciprocals of these numbers.
- Clear out fractions by multiplying by an appropriate constant, and divide by any common factors to obtain the lowest possible integers.

A single specified plane is referred to as (*hkl*) (see Figure 10). All equivalent, parallel planes are represented by the same set of indices. Thus the planes whose intercepts of are x, y, z; 2x, 2y, 2z; 3x, 3y, 3z, etc., are all represented by the same set of Miller indices. A family of planes related by the crystal symmetry is referred to as {*hkl*}.

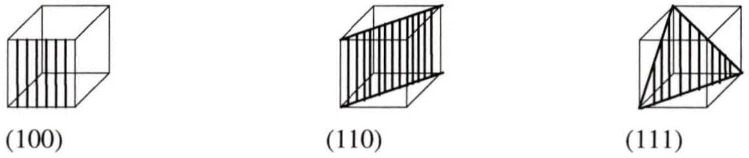

Figure 10. Miller indices of important crystal planes.

2.3 *Crystal imperfections*

The "perfect" crystal does not exist. All real crystals contain defects, which disturb the perfect lattice. These defects are only a very small fraction of the whole crystal. However, they may have a significant influence on the physical properties of crystals, namely optical, electrical and mechanical properties. It is therefore essential to understand and measure these defects. All possible crystal defects can be divided into three categories (Faktor, 1974): point defects, line defects and area defects.

There are two basic single point defects: the vacancies and the interstitial atoms. The interstitial atoms occupy positions between the lattice sites. A vacancy forms when the atom at a lattice site migrates to a free surface. If a pair of vacancy and interstitial occurs, it is called a Frenkel pair (see Figure 11). The concentration of such defects in a crystal depends on the free energy of formation of the defect. These defects are thermodynamically stable and are present in all crystals.

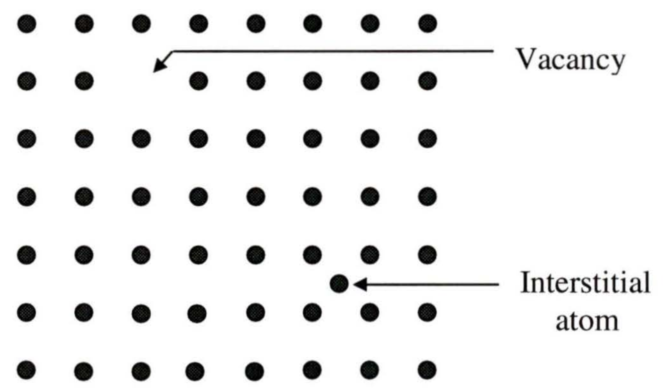

Figure 11. Interstitial atoms and vacancies.

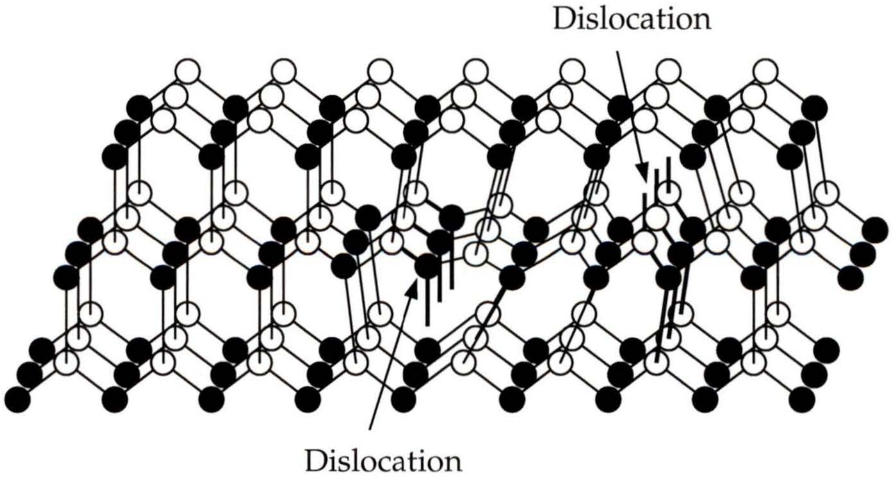

Figure 12. Dislocations in zinc-blende structure.

There are two elementary types of dislocations: the pure edge dislocation (see Figure 12) and the pure screw dislocation. The pure edge dislocation may be thought of as the edge of an extra half-plane of atoms inserted in the crystal. The screw dislocation results from shearing the lattice. These dislocations are thermodynamically unstable. They are formed during the crystallization process when the crystal is subject to stress, usually because of thermal gradients, and crystal planes start slipping one another. These dislocations cannot readily be removed because of certain critical shear stress. All real crystals contain such defects. Dislocations are often responsible for device failure, causing current leaks and breakdown of the p-n junction. They can reduce the yield of a circuit, cause non-uniformity of the threshold voltage, and lower the reliability of devices. Thus, the density of the dislocation must be kept below a certain level.

The planar defects include stacking faults, grain boundaries and twinning as well as twin planes. A stacking fault is produced when the sequence of perfect lattice stacking planes is disturbed. If perfect stacking planes are in a regular order ABCABCABC…, now the sequence becomes ABCACABC or ABCACBCABC. A B-plane is missing in the first case and an extra C-plane is inserted in the second case. This also results in the twinning in the crystal.

A grain boundary separates two regions of single crystals of different orientations. If the lattices on either side of the grain boundary are in a special orientation to one another, the crystal is said to be "twinned" and the boundary is called a twin boundary. Twinning is common in II-VI semiconductor materials, because of their low stacking fault energy. The twining surface in CdTe is always {111} planes, and the {111} planes turn 60° along the axis of <111> direction.

Most volume defects are critical, which result in failure in semiconductor devices. Volume defects include crystal orientation, structure and composition.

If a crystal contains a series of grains in different orientations, this crystal is polycrystalline. All semiconductor crystals grown for device applications are required to have a single crystal structure.

If one crystal contains even two different structures, it is useless for device applications. The properties are totally different if the structures are different for the same kind of single element, as diamond and graphite consist of carbon element but in different structures.

The defects of chemical composition are known as precipitates and inclusions, although the difference between precipitates and inclusions is not always distinguished. However, the creating mechanism and the size of precipitates and inclusions are different (Rudolph, 1995). The precipitate size in CdTe crystal will not exceed 10-30 nm, and particles with sizes over 1 μm should be inclusions.

The inclusions and precipitates are detrimental to the optical transmission devices like x-ray detectors, and thus, they must be kept to a minimum.

Chapter 3 Physics of CdTe/CdZnTe Semiconductors

3.1 Structure and Bonding

CdTe belongs to the zinc-blende structures. Its unit cell is a face-centered cube. The zinc-blende structure is similar to that of diamond. Its symmetry, however, is lower than that of diamond, which consists of only one kind of atom-carbon. The zinc-blende structure consists of two kinds of atoms. Figure 13 shows the CdTe crystal structure whose vertices and centers of faces are occupied by Cd (Te) atoms, and four out of the eight tetrahedral interstices are occupied by Te (Cd) atoms. Each Cd atom is surrounded by four Te atoms, and each Te atom is surrounded by four Cd atoms.

Bonds between atoms are the attractive interatomic forces that are responsible for the stability of the crystal. There are three main types of bonding: ionic bonding, covalent bonding, and metallic bonding. Covalent bonding and ionic bonding are important for those elements in IV, III-V and II-VI of the periodic table. All group IV materials are covalent crystals, like Si and Ge. Crystals of III-V and II-VI are mixtures of ionic and covalent types. This is because the average number

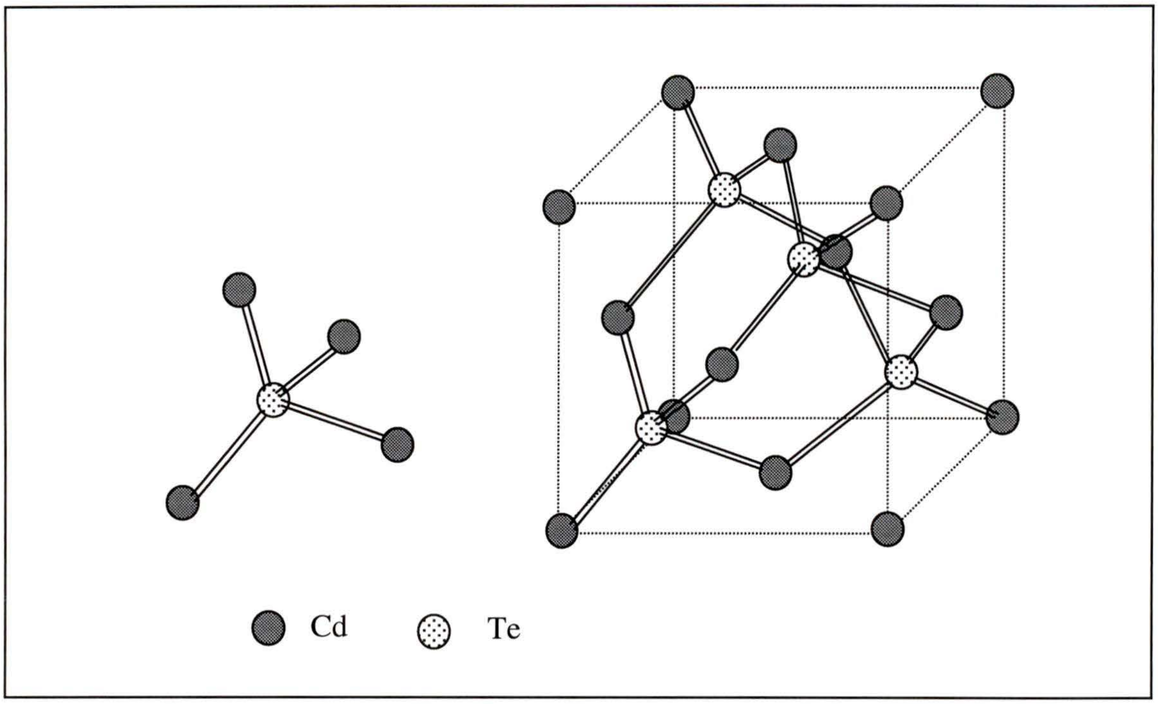

Figure 13. CdTe crystal structure.

of electrons per atom is still 4, but group VI atoms are considerably more electronegative than group II atoms, thus introducing ionicity. The ionic contribution varies considerably over the whole compound semiconductors. In CdTe, the ionic contribution to the bonding energy is one of the largest among tetrahedrally coordinated semiconductors. It is about 70% ionic contribution to whole bond energy in the CdTe crystal, 58% in ZnTe and 30% in GaAs (P. Rudolph, 1995). Usually, the ionic bonding is stronger than other kinds of bonding. This strength is attributed to the strength of the Coulomb force responsible for the bonding; the valence electrons bond rather tightly to the lattice atoms. Thus, the energy band gaps of these compounds are larger than those of covalent semiconductors with comparable atomic weights, although their hardness does not match that of covalent semiconductors. Covalent crystals tend to be hard like diamond, and incapable of appreciable bending. Any attempts to alter them are strongly resisted by the crystal. The ionic bonding contribution of CdTe may be the main reason for the differences between properties of CdTe and the other zinc-blende semiconductors.

3.2 Thermodynamics of Cd-Zn-Te ternary systems

The understanding of the phase relations of CdTe/CdZnTe and ZnTe is the most important step in growing high quality CdTe/CdZnTe crystals from melt. These relations provide the basis of the growth techniques. The electrical and optical properties of crystals strongly depend on the deviation from stoichiometric growth. High point defect density is also the result of the nonstoichiometric growth. Therefore, the control of crystal composition during the crystallization is extremely important for both the physical properties and defect structures of the crystal. Figure 14 (P. Rudolph, 1994) gives the phase relation of temperature versus composition. In earlier studies for CdTe, many authors believed that the melting and freezing arrest for CdTe is 1092°C (J. Steininger, 1970. M. R. Lorenz, 1962). Presently, it is found that the stoichiometric CdTe melt point is lower than 1092°C. From the phase relation of T-y, it can be seen that the congruent melting point T_{cmp} (1092°) deviates from stoichiometry by about $\delta y \approx 6\times10^{-4}\%$ ($\approx 1.5\times10^{17}$ Te excess atoms per cm^3) on the Te-rich side. An exactly stoichiometric CdTe melt does not solidify at the maximum melting point T_{cmp}, but at a lower equilibrium temperature that is equivalent to the intersection point between the

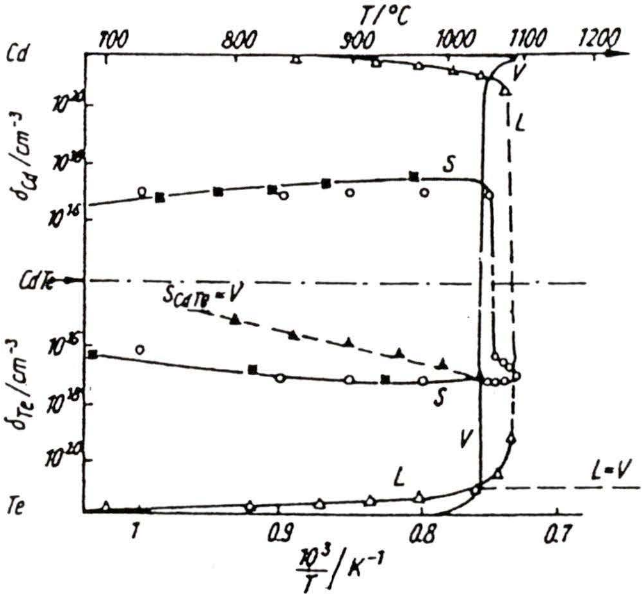

Figure 14. The phase relation of temperature versus composition (Rudolph, 1994).

liquidus and the stoichiometric line. This temperature point is considered to be between 1062°C and 1077°C in the Cd-rich side by P. Rudolph and his colleagues.

To obtain stoichiometric CdTe, excess Cd (about 10^{-3} % in the melt) is necessary. The vapor pressure of Cd is about 2×10^{5} Pa. In the VGF or Bridgman techniques this pressure can be controlled by a Cd reservoir with a constant temperature. The temperature of the Cd source can be estimated by the phase relation of p-T or by following relations (P. Rudolph, 1995; K. Hultgren, 1973, J. P. Schwartz, 1981 and N. Yellin, 1985):

$$\log P_{Cd}\,(\mathrm{atm}) = -5808/T + 5.956 \qquad T<594K$$

$$\log P_{Cd}(\mathrm{atm}) = -5317/T + 5.119 \qquad T>594 \qquad (1)$$

$$\log P_{Te2}(\mathrm{atm}) = -5960.2/T + 4.7191 \quad T>723K$$

or

$$\ln P_{Cd}\,(\mathrm{atm}) = -13859/T + 26.15 - 1.8415 \ln T \qquad (2)$$

Different deviation from stoichiometric CdTe growth on the Cd-rich side can be manipulated to obtain CdTe with needed the electrical and optical properties by controlling Cd vapor pressure (that is by controlling the temperature of the Cd reservoir). The temperature of the excess Cd reservoir should be between 780°C and 825°C (767°C is the boiling point of Cadmium); the vapor pressure is correspondingly between 1.2×10^5 Pa and 2.5×10^5 Pa. The analysis is done only for the Cd-Te binary system. Data available on Cd-Zn-Te ternary systems are limited. The only data, obtained by Steininger et al, are given in Table 3 (J. Seininger, 1970). When 10% Zn is in the compound, the arrest temperature is 1121.6 ± 0.6°C, and when 20% Zn is in the compound, the arrest temperature reaches to 1156.6°C. The melting point of ZnTe is 1290° ± 2°C.

There is a lack of data in the literature for phase relation of the Cd-Zn-Te ternary system. Therefore, we must assume that the information available about the excess Cd reservoir in an Cd-Te binary system can be used for a Cd-Zn-Te system. This is a reasonable assumption, because the Zn partial pressure is low, and the amount of Zn in the CdZnTe alloy is small. The maximum Zn percentage in the CdZnTe alloy will be 10% in our experiments.

Table 3. Cd-Zn-Te experimental thermal analysis data.

Zn	Cd	Te	Arrest temperature,	Reproducibility,°
0.10	0.40	0.50	1121.6	±0.6
0.175	0.325	0.50	1144.5	---
0.20	0.30	0.50	1156.6	---
0.25	0.25	0.50	1176.1	±0.1
0.30	0.20	0.50	1198.1	---
0.40	0.10	0.50	1244.9	±0.2

3.3 Properties of Liquid CdTe

Unlike the III-V materials, the II-VI semiconductors have some special properties in the molten state. When CdTe is slowly superheated, the dissociation coefficient is assumed to be roughly 0.05 (P. Rudolph, 1994). However, in the case of GaAs, the melt state is characterized by the dissociation coefficient of 0.9. This is the most significant difference between CdTe and GaAs. The liquid behaviors of CdTe and GaAs are also different. After Glazov et al (V. M. Glazov, 1969) studied the electrical and magnetic properties of CdTe 60 K above the melting point, it was found that the molecular state in stoichiometric Cd-Te melts is stable. Therefore the solid-melt transition should be:

$$\text{Solid semiconductor} \Leftrightarrow \text{Liquid semiconductor} \qquad CdTe^{S} \Leftrightarrow CdTe^{L}$$

While the solid-melt transition of GaAs is

$$\text{Solid semiconductor} \Leftrightarrow \text{Metalic liquid} \qquad GaAs^{S} \Leftrightarrow Ga^{L} + As^{L}$$

Figure 15, Figure 16 and Figure 17 show the experimentally measured temperature dependencies of the electrical conductivity σ_e, magnetic susceptibility χ_m and kinematic viscosity ν of the CdTe melt obtained by Glazov et al. "The low value of σ_e and the increasing temperature function indicate a typical semiconductor behavior of the molten state. However, the electrical conductivity rises rapidly at the melting point due to the release of free carriers caused by an increasing effect of metallisation. The steeply decreasing temperature functions for χ_m and ν also emphasize the associative melt character at moderate overheating".

This semiconductor-like behavior of a slowly superheated CdTe melt was explained by Glazov et al and P. Rudolph as: "The spatial character of the covalent bonding gives rise to the molecular structure and can be expected to assist in the formation of three-dimensional (tetrahedral) and two-dimensional (rings, chains) associates. With rising temperatures (superheating) these complexes will be increasingly broken down. The melting process in CdTe crystals first of all begins with splitting along the {110} faces quickly reforming into <110> chains in liquid." In other words, the <110> chains and molecular structure may exist in slowly superheated molten CdTe, but the exact structures in the liquid CdTe are still unknown.

The semiconductor behavior of liquid CdTe makes the thermal history of the melt an important parameter in the growth of single crystals. This is because there is a specific relationship between superheating and supercooling.

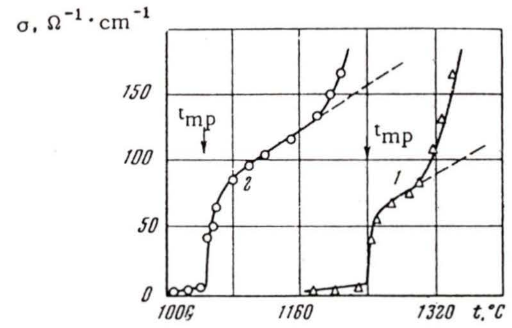

Figure 15. The electrical conductivity of ZnTe (1) and CdTe (2) (Glozov, 1969).

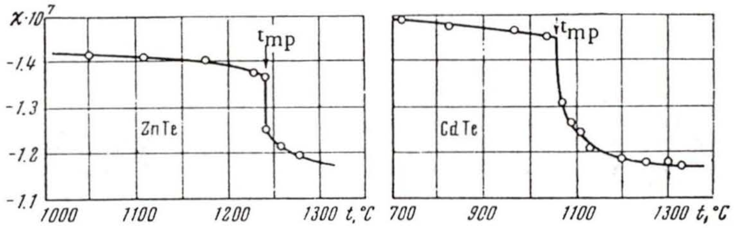

Figure 16. The magnetic susceptibility of ZnTe and CdTe (Glozov, 1969).

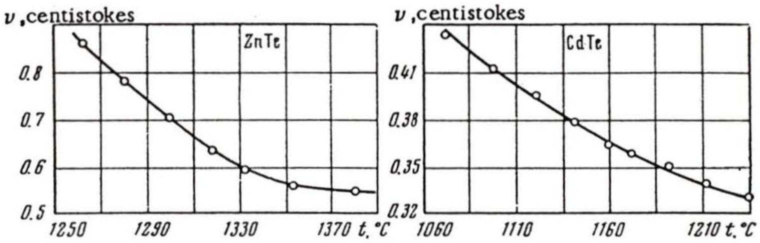

Figure 17. The kinematic viscosity of molten ZnTe and CdTe (Glozov, 1969).

Supercooling is one of the most detrimental phenomena in the melt growth of CdTe crystals. When superheating is 10 K, three-dimensional complex particles in the liquid CdTe transit to lower dimensions of melt associates. Supercooling is expected to occur because more energy is needed to form nucleation (P.

Rudolph, 1993). During the growth, this supercooling makes the solid-liquid interface jump up suddenly after travelling for several centimeters, making the first part of the ingots highly polycrystalline. However, the part following the first polycrystalline section is a single-crystal region or a region with only one or two grain boundaries. When superheating is less than 10 K, no supercooling occurs and a larger number of grain boundaries and twins are originated after a single crystal initial growth. The crystal quality is almost the same for the whole CdTe ingot without supercooling. High superheating is detrimental for the first-to-freeze region and good for growing large grain crystals after the tip region.

3.4 Other properties of CdTe/CdZnTe

The lattice parameters of $Cd_{1-x}Zn_xTe$ depend on composition x (see Table 4. M.Schenk, 1996). The lattice parameters range from 0.6482 nm to 0.6103 nm as x goes from 0 to 1. Other properties are shown in Table 5.

Table 4. Lattice parameter a of $Cd_{1-x}Zn_xTe$ on composition x.

x ±0.01	0	0.040	0.205	0.49	0.705	1
a ±0.00024 nm	0.64822	0.64652	0.64079	0.62928	0.62163	0.61033

Table 5. Properties of CdTe.

Density	Thermal Expansion		Bandgap
5.68 g/cm^3	$5.0 \times 10^{-4}\ K^{-1}$		1.56 ev
Band	Mobility (cm^2/V-s)		Dielectric Constant
Direct	Electron	Hole	10.2
	1050	100	

Chapter 4 VGF Apparatus and Crystal Growth

This chapter presents the VGF growth technique and its setup in detail. First, a general discussion is given on certain features of the growth process, and then the experimental setup, which was originally built for an LPEE growth of III-V materials, is described in detail. This is followed by a discussion on the influence of ampoule shape on the quality of grown crystals. Finally, the procedures of material (Cd, Zn, and Te) and ampoule preparation, and the details of the growth process are presented.

4.1 General consideration

4.1.1. Control of Cd pressure

The partial pressure of Cd plays an important role in growth of CdTe/CdZnTe crystals. Crystals grown with different Cd pressures may possess different properties. Single element materials, i.e., Cd, Te and Zn, in single-element forms have different vapour pressures. The vapor pressure of Cd is much higher than that of CdTe/CdZnTe compounds. The first step, an important step, in crystal growth is to obtain the compounds from the reaction of single-element materials. This process is called "synthesis". The vapour pressure of Cd exceeds 13 atm at the melting point of compound CdTe/CdZnTe. The experimental apparatus was not designed to stand such a high pressure. Due to the possibility of explosion, the use of totally high temperature reaction in the whole ampoule was ruled out in our experiments. Setting the reaction temperature below the melting point of the compounds, as is done in the phase transfer method, would have eliminated the possibility of explosion, but in this case the synthesis process would have taken very long. In order to overcome these difficulties, a method of "Cd-reservoir" is employed in our experiments. The technique is as follows. First, the reaction region of the tube is kept at a temperature above the melting point of the compound, which is between 1120° to 1160° C. At the same time, the other end of the tube is maintained at a relatively low temperature (about 785-825°C). In such an arrangement, the cool end of the tube serves as a reservoir of Cd, and the temperature of the reservoir determines the Cd partial pressure. In the hot region of the tube, the single-element materials are melted and react. This arrangement, i.e., maintaining a part of the tube lower than the melting temperature of the compound, reduces the risk of explosion during the reaction of elements. However, this Cd- reservoir technique is also very beneficial during the growth process since the excess Cd vapour could be released into the reservoir.

4.1.2. Superheating and supercooling

As stated earlier, when the melt begins to solidify without supercooling, single-crystal grains tend to form in the very beginning. Superheating is usually the cause for supercooling. Experiments show that in growth of CdTe, supercooling cannot occur if the superheating does not exceed 10°C. This suggests that the melt should be kept within this superheating limit if one wishes to initiate the growth with a single crystal at the tip of the tube in the very beginning. However, experiments conducted by other researchers show that the growth of large-size single crystal grains is very difficult when the melt is kept under this superheating limit. On the other hand, experiments also show that, although the melt of high superheating can lead to supercooling resulting in polycrystalline growth in the beginning, it is possible to grow large-size single crystal grains following a polycrystalline growth at the tip.

We investigate here the possibility of combining these two opposite processes to grow large-size single crystal grains throughout the entire ingot. The basic idea in our experiments was to control the temperature profile such that the melt near the tube tip is kept below the superheating limit of 10°C, and therefore no supercooling could occur during solidification. At the same time, the melt above the tip area is maintained at a temperature profile of relatively higher superheating. Controlling it in this way, when the temperature of the tip region goes below the melting point, a single crystal can begin to grow from the very beginning. Then the melt above the tip, which has a higher superheating temperature profile history, favors the growth of large-size single crystal grains when the temperature profile moves down. At the end, large size single crystal grains can be obtained through the entire volume of the ingot. The development of this experimental technique to grow large crystals by the VGF technique is one of the most important contributions of this study.

4.1.3. Binary and ternary crystal growth

In order to gain some experience and insight, and also to avoid the complexity of a ternary growth at the begining, the above-described process was first implemented to a binary system (CdTe). Then, the experience gained through the binary growth was used for the ternary crystal growth of CdZnTe. In the ternary growth, further consideration was necessary for the melting points of CdZnTe, the influence of Zn composition, and the complex phase transitions of ternary compounds.

4.1.4. Choice of Zn composition ratio in the CdZnTe compound

For the case of $Cd_{1-x}Zn_xTe$ compounds, materials properties of grown crystals depend very much on the value of the Zn composition ratio x. For different x values, grown crystals will have very different properties. The selection of the Zn composition is therefore very important. Based on the requirements of potential device applications, two composition ratios are selected for the experiments: $x = 0.04$ and 0.10. Each Zn composition will require a different temperature profile. Although the temperature profiles of the two cases have the same shape, the profile for the compound of higher Zn ratio is shifted up, compared with the one of lower Zn ratio.

4.1.5. Trade-off between crystal quality and growth time

Synthesis and crystal growth are usually two separated processes. Both take considerably long time. In order to investigate the trade-off between the crystal quality and the total growth time, in our experiments, we attempted to combine the synthesis and growth processes into one single process while still treating two processes separately.

4.2 The furnace and its base platform

The schematic of the VGF apparatus is presented in Figure 18. The furnace is tubular in form, with three independent heating zones. The dimensions of the furnace are given in Table 6. The maximum temperature of three zones is 1200°C. Temperatures of the zones are controlled by three separate controllers which can be programmed by a computer. They can also be controlled without a computer. One controller is a master controller; the other two are slave controllers. Selected temperature profiles can easily be changed and controlled. A quartz tube the diameter of which is the same as that of the inside diameter of the furnace is placed inside the furnace in order to keep the system clean and also protect the furnace. The quartz tube is selected because of its material properties such as high melting point, and low thermal expansion coefficient within the growth temperature range.

One end (the lower end in the vertical position) of the furnace is insulated to maintain the crystal growth section inside the furnace at desired high temperatures. The other end is closed by an aluminum cover. Inside the aluminum cover, a copper water cooling tube is attached to an outside water cooling system to keep Zone 1 at relatively low temperatures (see Figure 18). During the growth, a constant temperature point is established in Zone 1. This point is used to control the Cd pressure inside the ampoule. Two buffers are used inside the furnace to eliminate the heat transfer between Zone 1 and Zone 2. This is necessary because crystal growth occurs between Zone 2 and Zone 3, and the highest temperature of Zone 2 is 1160°C while the temperature of Zone 1 is maintained at a constant point between 785-825°C. The furnace is mounted on a rotating plate that can rotate 180° freely about the horizontal axis, and can be fixed at any angular positions. A sturdy aluminum base supports the rotating plate. The furnace can be used in horizontal or vertical positions, or any other positions between them. All the electrical cables (thermocouple readings, power lines for furnace) are fed from the ceiling. The entire platform is set on a concrete base that is isolated from the rest of the floor to prevent vibrations generated in other parts of the building.

Table 6. Dimensions of the furnace.

Over all length	743 mm
Length of zone 1	152 mm
Length of zone 2	305 mm
Length of zone 3	152 mm
Inside diameter	105 mm

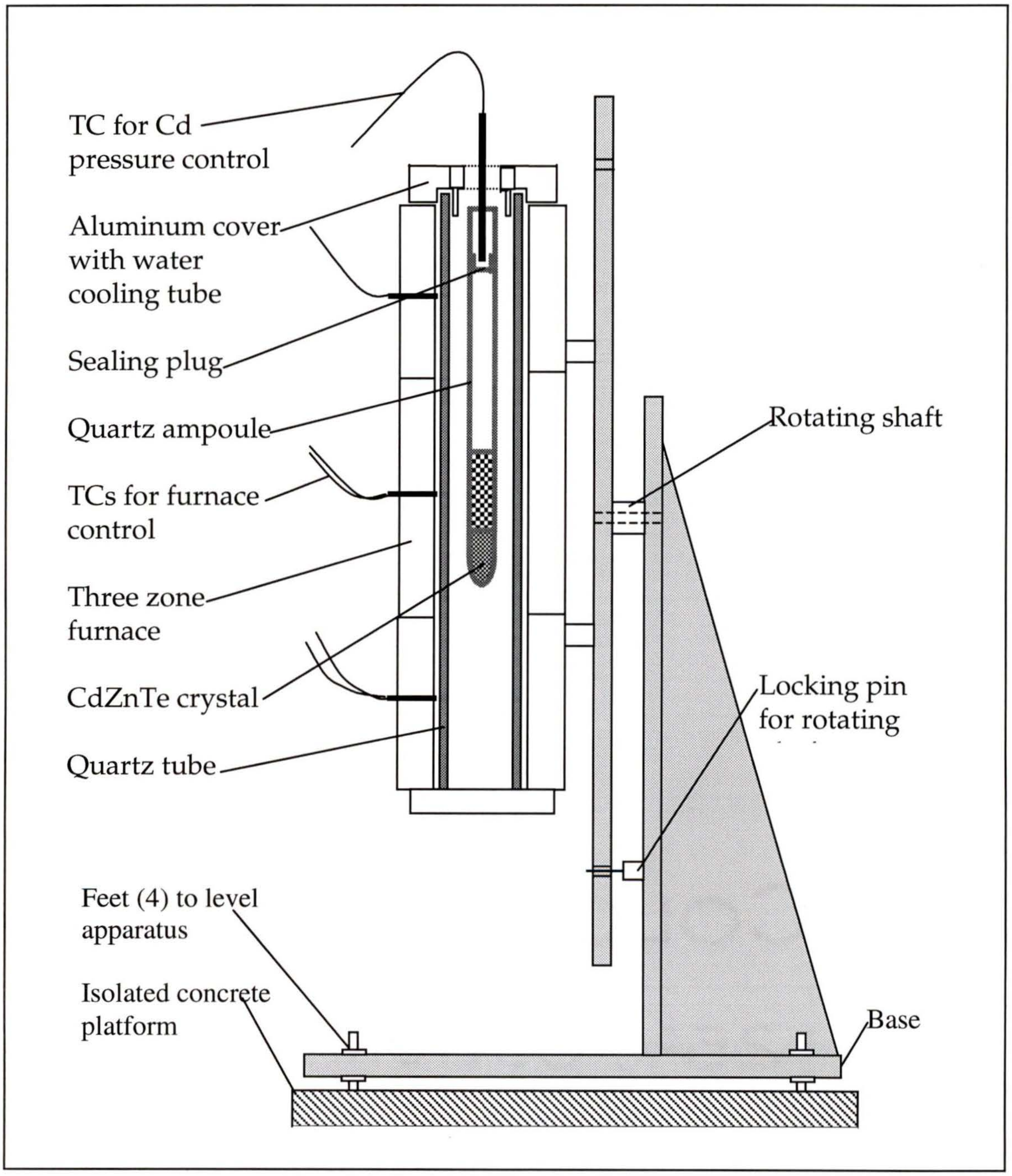

Figure 18. Diagram of VGF crystal growth platform.

4.3 Temperature profile of the furnace and ampoules

There are two thermocouples (TC) in each of the three zones of the furnace. One thermocouple is used to measure the temperature at the point of installation. The other one is for the control (alarm) purpose; if the system temperature exceeds the pre-selected temperature level, the power of the furnace shuts down automatically. The thermocouples are K-types, meaning that the junction is made of nickel-chromium and nickel-aluminum alloys. The temperature range of K-type thermocouples is between -200°C and 1260°C, i.e., the working temperature is almost at the upper limit of thermocouple temperatures. The gradient-freezing configuration and the temperature profile are shown in Figure 19. The temperature is measured along the axis of the furnace. The temperatures of Zone 2 and Zone 3 are respectively set to 1150°C and 1100°C. The temperature of Zone 1 is set to 800°C. It can be seen in this temperature profile that the best region to grow crystals is between 24th cm and 32th cm measured from the end of Zone 3. The Cd pressure control region is between 60th cm and 65th cm.

The ampoule is placed in the furnace such that the tip of the quartz is at the point of 1110°C while the top section of the ingot is at the temperature of 1125°C. In this way we establish approximately a 10°C superheating at the tip region of the molten CdTe/CdZnTe, and a 25°C superheating at the top region of the molten

CdTe/CdZnTe. Considering the relationship among the superheating, supercooling and crystal quality (see Chapter 3), one can see that this selected temperature profile encourages single crystal growth at both the tip region and also the region following the tip.

The selection of ampoules, in the sense of both shape and material, is one of the most important steps in any growth process. This is also true for the VGF technique. An ideal crucible material must:

- have smaller thermal expansion than that of the crystal to be grown,
- release minimum amount of impurities to the melt, and
- permit easy removal of the ingot after growth.

Considering these requirements, ampoules made of graphite, boron nitride (BN), pyrolytic boron nitride (PBN), and quartz are acceptable. However, the following further favorable properties of quartz convinced us to select quartz ampoules as crucibles.

The interaction between molten CdTe and quartz was studied by R. Shetty (Shetty, 1990) et al. The surface tension of molten CdTe decreases with increasing temperature, and is, at 1092°C, about 170-190 dynes/cm with different Cd over - pressures. The contact angle of molten CdTe on the quartz surface is a function of temperature. The degree of wetting increases with increasing temperature. The contact angle at the melting point (1092°C, with excess Cd of $\rho \approx 2.3\text{x}10^{-3}\text{g/cm}^3$) is

83° on plain quartz and 90° on HF-etched quartz (Shetty, 1990). Such a large contact angle implies that there will only be slight wetting on the quartz ampoule (see Figure 20). In addition, quartz has a high melting point, a low thermal expansion coefficient and a high resistance to oxidizing. It is transparent, i.e., allows visible observation, and finally it can be obtained at low cost.

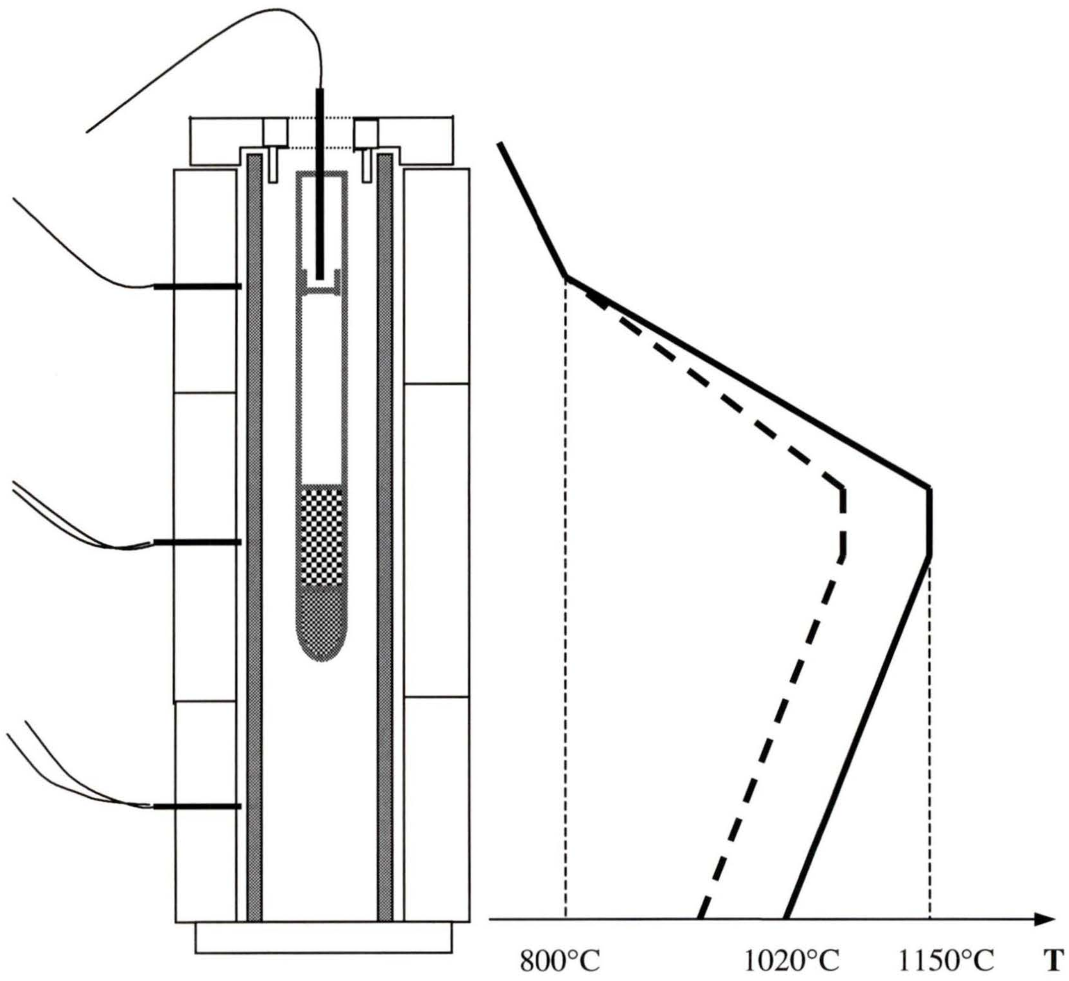

Figure 19. Gradient Freezing Configuration.

The ampoules of two different tip configurations are used in the experiments (see Figure 21). The first type has a spherical tip while the second one is of conical tip of 120° angle. The inside and outside diameters are respectively 26 mm and 30 mm, and thus its thickness is 2 mm. The total length of the ampoules is 57 cm. There is a sealing plug inside of the ampoule at the location 40 cm from the tube end. The single element materials are loaded into the tube, and then the tube is vacuumed and sealed by the sealing plug at this location. This location of the tube is maintained at constant temperature and is used to control the Cd pressure during the synthesis and crystal growth processes.

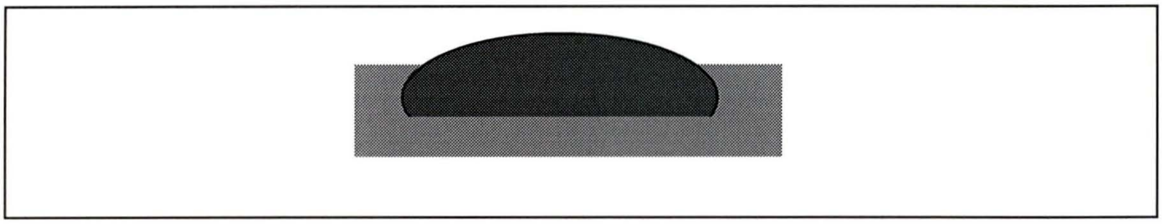

Figure 20. Sessile drop of molten on quartz at 1096°C.

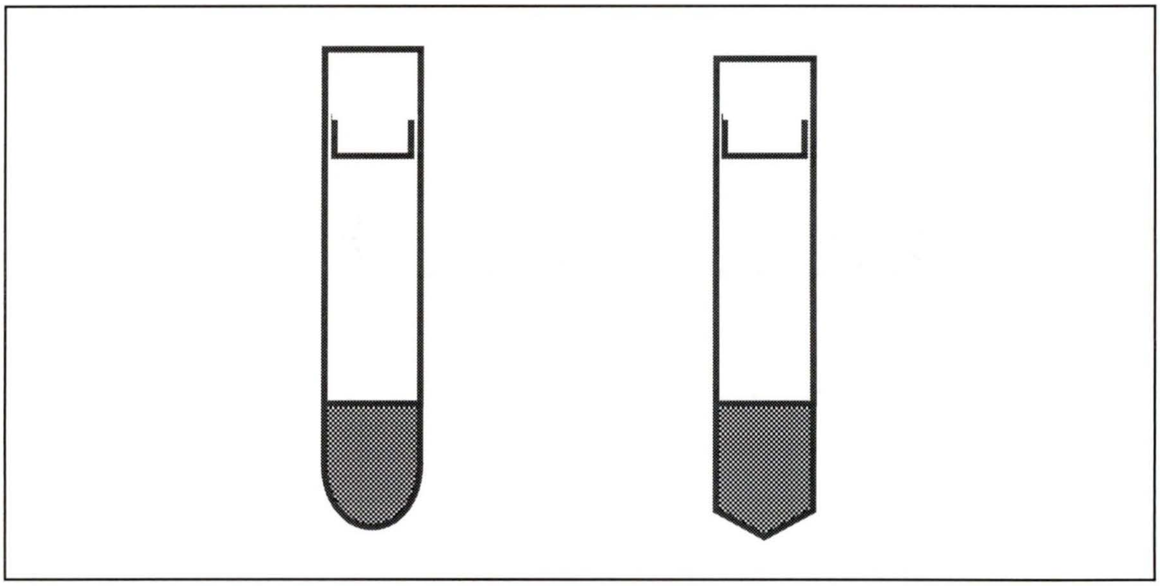

Figure 21. Ampoule shapes.

4.4 CdTe/CdZnTe crystal growth processes

The quality of grown CdTe/CdZnTe crystals strongly depend on the preparation process of materials and ampoules. Thus, the required steps in this process must be carried out very carefully. A typical preparation process is as follows. First, the quartz ampoule is treated with a $HCl + HNO_3$ mixture for 2 ~ 3 hours. After this acid etching, it is rinsed with flowing water for 24 hours. Then, the ampoule is baked for 8 hours at 800°C to remove molecules attached on the inside surface of the tubes. After baking, the quartz tube is ready for use. The single element materials, i.e., Cd, Te, and Zn, are synthesized from high purity 6 nines (6N) Cd, Zn and Te, obtained from Noranda Advanced Materials (their impurity analysis is given in Appendix 3). Cd and Zn elements are subjected to an ultrasonic cleaning with acetone and methanol, and then their surfaces are treated using the etchant $HNO_3 + H_2O$. Cd and Zn are then loaded into the ampoule. Then, Te is cleaved and removed from Ar sealed packages, and immediately loaded into the ampoule without any acid etching or cleaning treatment.

Cd, Te, and Zn are weighed in a stoichiometric ratio before loaded into the ampoule. Taking into account the Cd vapor pressure at high temperatures, extra Cd is added to compensate for the loss of Cd during the processes. Te_2 partial pressure is neglected because the Te_2 contribution is less than 4% in the total vapour pressure.

After Cd, Te and Zn are loaded into the ampoule, the ampoule is connected to the pumping system. When the vacuum is up to 10^{-5} mbar, the ampoule is then sealed and is put into the quasi-horizontal gradient freezing furnace for synthesis. The ampoule position inside the furnace, and the angle between the axis of furnace and the horizontal are shown in Figure 22. The furnace is set in a position so as to make full use of synthesis space and to keep the Cd vapor-control point at a relatively low temperature. Single element materials are kept in the section where the highest temperature is between 1100°C and 1160°C. The materials are then heated very slowly up to 800°C. (The rate of heating is very important, temperature must be risen very slowly to avoid any explosion. V. M. Glazov (Glazov, 1969) stated that "Cd and Te react violently even at temperatures as low as 350°-360°C while Zn and Te react at 550°C-570°C, to form compounds in the form of a loosely packed porous mass with local unreacted regions"). The materials are kept at 800°C for 24 hours to ensure complete reaction. Then the temperature ramps continuously up to 1160°C. After holding several hours at this temperature, the melt is solidified by quickly cooling down to room temperature. At this point the ampoule and the solid compound are ready for the VGF growth process (see, Figure 24).

During the growth process, the furnace is set in the vertical position (see Figure 23). The temperature profile is moved gradually, lowering the temperature below the melting point of the compound material. Freezing begins at the tip of

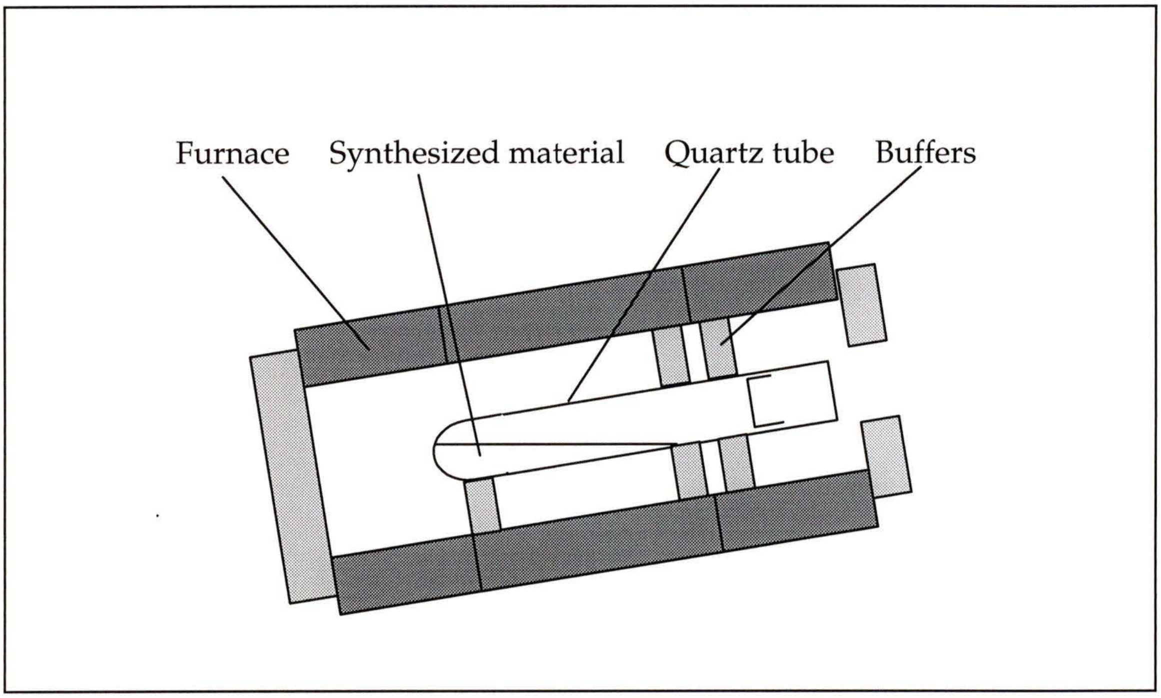

Figure 22. The furnace position during synthesis.

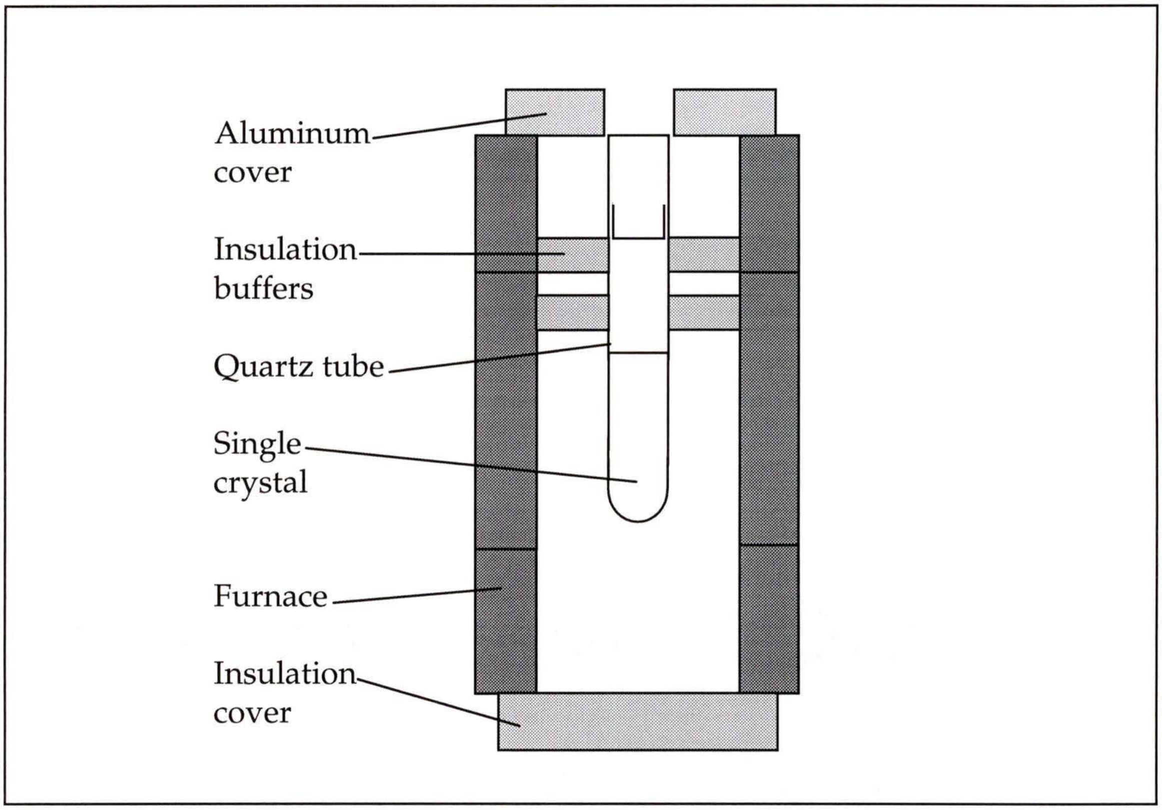

Figure 23. The furnace position during crystal growth.

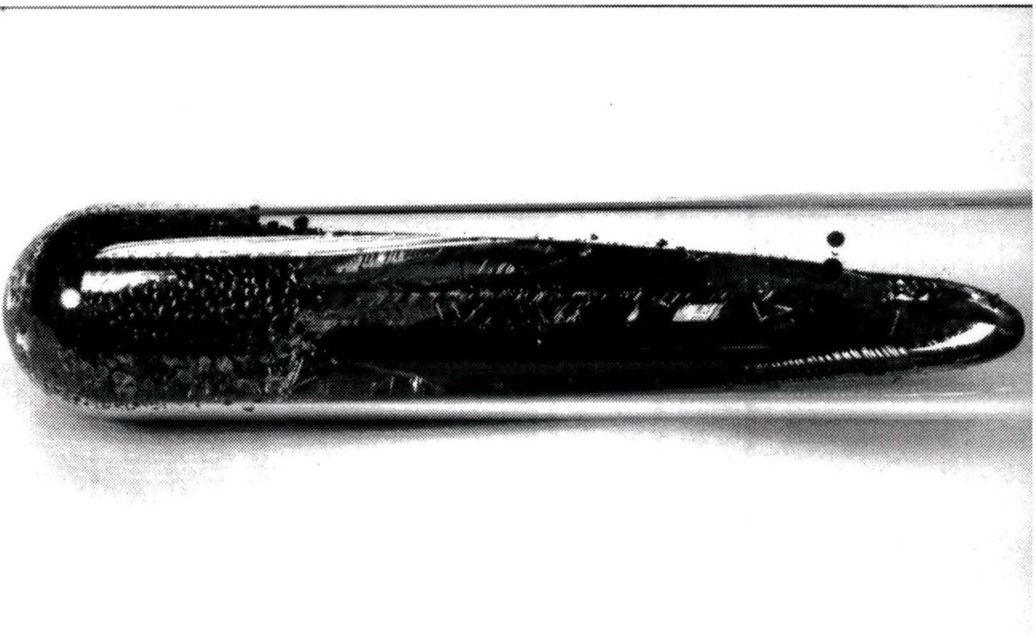

Figure 24. Synthesized materials.

the ampoule and gradually grows to form an ingot. The temperature of the Cd reservoir is controlled between 825°C and 785°C, corresponding to the Cd vapor pressure between 2.1 atm and 1.25 atm. The axial temperature gradient is 2.3°C/cm at the growth interface. This low gradient was selected to reduce the thermal convection in the melt, to minimize the curvature of the solid/liquid interface and also to reduce the thermal stresses on the solidified portion of the ingots. The cooling rate is about 0.6°C/hour during the growth process. The growth rate is 2.5mm/hour. After solidification, the ampoule is cooled down to 800°C at a rate of 20°C/hour and then down to room temperature at a rate of 40°C/hour.

In the experiments, two methods were used:

(1) One step method. The synthesis of single elements is performed in the horizontal configuration. The furnace is then rotated to its vertical position while the compound material is still at its melt condition (1160°C), and then the growth is started. The one step method combines synthesis and growth together. It is effective and efficient, and saves time.

(2) Two step method. The synthesis process is completed in the horizontal position. Then, the solid compound is melted again quickly in the vertical furnace, and the growth is initiated. The duration of the growth process is much longer than the one-step method. As we will discuss later, the difference between these two methods is significant.

4.5 The ingot analysis

Eight VGF experiments were conducted to grow CdTe/CdZnTe alloy crystals without seeding. In each run, slightly different growth conditions and different amount of single materials were used. Table 7 summarizes the experimental data used. Three sets of experiments were conducted, namely, the synthesis and growth of compound CdTe, and CdZnTe ternary alloy with 4% Zn and 10% Zn contents. The results of these series of experiments are also presented in Table 7. As can be seen from the table, the two-step method yielded better quality ingots compared with those from the one step method, in terms of both thermal stress and cracks distributions. In addition, the ingots grown by the two-step method were easily slid out after the tube is cut and opened. The surfaces of the ingots were shiny and smooth, and there were no visible impurities and cracks on the surface of the ingots.

The first run was carried out using an ampoule with a spherical tip. Ampoules with a conical tip of 120° angle were used in the second and third runs to increase the possibility of single crystal growth in the very beginning. It was found that a tube with a conical tip tends to be broken during the cooling stage (below 800°C) following the growth. Therefore, quartz tubes with spherical tips were used in the next five experiments.

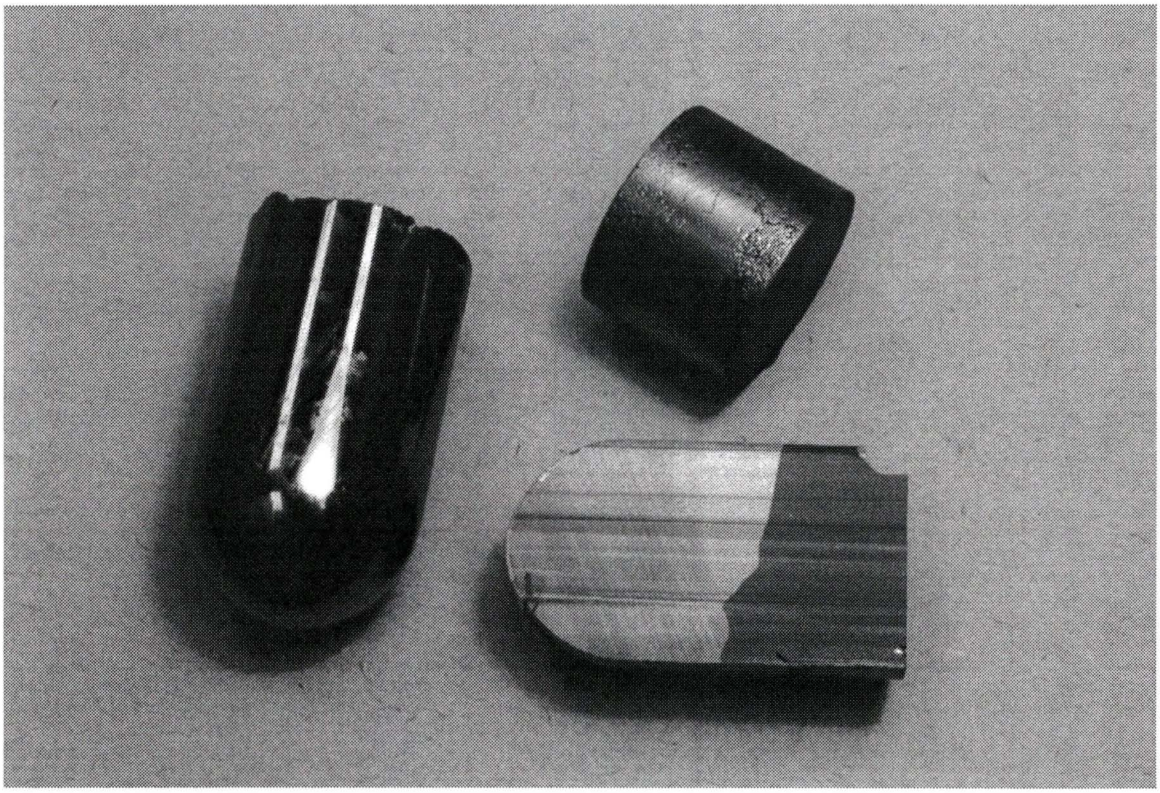

Figure 25. CdTe/CdZnTe ingots.

Figure 25 shows the CdTe/CdZnTe ingots obtained by the VGF technique. The ingots are 26 mm in diameter and about 50-60 mm in length. Large single crystal grains can be seen clearly on the surface of cross-section of the ingot.

Some cracks can be seen on the ingots from run 02 to run 06 (one step method). Especially, the ingots of run 05 and 06 were broken at the tip region. The reasons for these breaks are believed to be the following:

(1). Second-phase materials are trapped inside the solid crystal. When temperature decreases, the second phase materials expand and become solid. The expansion makes the crystal break. It becomes worse when the trapped liquid contains other single elements, like Te inclusions with some Cd molecules inside them.

(2). Stress of the crystal is too high. The presence of stresses relates to non-linear temperature distribution in crystals and the subgrain structures in the CdTe/CdZnTe crystals. Stress in crystals is a common problem since a temperature gradient is required to grow crystal from the liquid phase.

One tube was broken at the sealing plug during crystal growth stage at run 04, because the thermal couple used to control Cd vapor pressure gave an erroneous temperature reading (the actual temperature was 100°C higher than the reading temperature). The actual temperature was around 900°C, while the boiling point of the Cd is 767°C. The pressure of Cd at 900°C is 3.75 atm and the quartz ampoule could not stand such high pressure. The sealing plug was broken at the growth stage, because the excess Cd was released when the molten CdZnTe became solid and the Cd vapor pressure kept increasing. 36.9% of the charged materials were lost at run 04. The lost materials were precipitated on the top of the cool region of the ampoule.

In Table 7, the statement of "good" ingot means that there is no obvious impurity and cracks on the ingot; the surface of the ingot is shiny and large grains can be seen on the surface.

Table 7 Data of a series of runs for CdTe/CdZnTe.

Crystal No.	Weight before loading (g)	Ingot Weight (g)	Extra Cd (g)	Cd reservoir T°C	Method	Result	Lost %
01	172	150	5.8	785	Two steps	Good	9.4
02	188	160	4.4	800	One step	cracks	12.6
03	187	158	7.8	800	One step	Strong stress	11.3
04	188	110	8.7	900	One step	explosion	36.9
05	184	173	6.3	825	One step	Stress	2.6
06	132	121	2.3	785	One step	Stress	6.6
07	132	116	2.5	785	Two steps	Good	10.2
08	130	123	1.8	785	Two steps	Good	4

The interface shapes between the liquid and solid phases were different in different runs. The typical interface shape is of concave surface, very close to a planar surface. The interface shape is very important because it is directly related to the quality of grown crystals. The selected temperature gradient, the growth rate and the geometry of the ampoule (Chong E, 1974) determine the shape of the interface. Thermal stresses are generally minimal for a planar interface. If segregation exists, for instance Zn in CdZnTe, the interface shape affects the compositional homogeneity of wafers obtained from the ingots. For instance, since the Zn composition will be the same along the interface, the planar interface will be the best for growing compositionally uniform CdZnTe crystals.

Chapter 5 Measurements of Characteristics

Following the synthesis and growth processes of CdTe/CdZnTe crystals in a VGF technique, the grown crystals were cut and examined for their mechanical (defect structures) and electrical properties. In this chapter, the results of the characterization of wafers obtained from the grown ingots are presented.

5.1 Sample preparation

In order to determine the properties of grown crystals, test samples have to be prepared using a special treatment. The steps of this treatment can be summarized as follows. First, the test samples have to be cut into wafers, along the <111>, <100> or <110> directions since they are the most important surfaces in applications. However, usually it is not easy to determine these directions for a raw ingot. Wafers are therefore normally cut perpendicular to the growth direction. Second, the wafer surface must be smooth and flat, and should be free of any scratches. Third, the surfaces must be fresh and free of any oxidized layers. Finally, the thickness and cutting speed have to be controlled carefully since the material is very brittle.

In our experiments, CdTe, $Cd_{0.96}Zn_{0.04}Te$ and $Cd_{0.9}Zn_{0.1}Te$ ingots were grown without seeding. In these ingots, we see that in most grains the angle between the growth direction and <111> direction is about 20° or 110°. It seems that these growth orientations are preferable to others. This observation agrees with the result obtained by Casagrande (L.G. Casagrande, 1993). Twinning can be clearly seen on the ingot surfaces, after the ingots were polished by fine sandpaper. A band saw was used to cut the ingots. The cutting rate is controlled at 1 mm per minute. The ingots were sliced perpendicular to the growth direction into a wafer of 2 mm thick. And then the slices were lapped and polished.

The lapping was done in three stages. First, the wafers were lapped by hand because of their irregular surface; then, wafers were polished by a polishing machine using 15 μm diamond powders and 1 μm diamond powders separately to remove the damaged layer caused by the cutting saw. The polishing area must be extremely clean because even a small particle as small as 15 μm could scratch the polished surfaces. Special attention must be paid when polishing diamond powders are changed from 15 μm to 1 μm. After 1 μm diamond particle polishing, the surfaces of the wafers showed no scratches and appeared smooth enough under a 100× microscope. After cleaning, they were etched by 5% Br + methanol or E solution (Inoue, 1962) for chemical polishing to remove the surface damage, because the surface damage also creates etch pits. Then, after thoroughly rinsed with methanol, the wafers were stored in methanol ready to be used for etch pit analysis and resistivity measurement.

5.2 Etch pit density

Etch pit density is an important specification to screen the quality of single crystal semiconductors. When CdTe/CdZnTe are used either as detectors or substrates for the epitaxy layer growth of HgCdTe (or MCT, used for IR array detectors), dislocation structures lead to fixed pattern noise and current leakage paths across the p-n junctions. Etch pits are found to correspond to dislocations in the crystals. The region around a dislocation usually is etched more rapidly than perfect crystal surfaces by certain acids and thus develops etch pits. Etch pit density analysis provides a simple tool of determining the number of dislocations that intersect the crystal surface. The term of etch pit density is often used synonymously with dislocation density, although some authors (Hahnert, 1994) indicated that etch pit density is smaller than the actual dislocation density. Dislocations in crystals are related to line defects. Figure 12 shows the situation of line defects. If these dislocations intersect the p-n junctions, they are actually the current leakage paths in the devices. Therefore, there is a maximum permissible dislocation density that would be acceptable for a stated application.

There are several solutions used for etch pits in CdTe/CdZnTe crystals, such as Nakagawa solution (Nakagawa, 1979), Everson solution (Everson, 1995) and EAg-1 solution (Inoue, 1962). Nakagawa solution only effects the (111) A surface. There are no etch pits appearing on other surfaces. The (111) A face in CdTe/CdZnTe crystals is the Cd or metal-rich face and the (111) B face is the Te-rich face. EAg-1 is selected in our case. The compositions of the solution EAg-1 and its related solution E are:

E solution: 10 ml of concentrated HNO_3 + 20 ml H_2O + 4g $K_2Cr_2O_7$

EAg-1 solution: 10 ml of E solution + 0.5 mg of $AgNO_3$

The E solution is used for chemical polishing before the EAg-1 solution is used for etch pit formation. The time for pit production is 60 sec. When the etching time is prolonged, the etch pits did not change their shapes and sizes. The etch pits were not distributed on the surface of the wafers homogeneously. Fluctuations in dislocation densities within a wafer exist. Etch pits are more pronounced at the ingot circumference (where the crystal is in contact with the quartz container) and the grain boundary than on the central region of the wafers (Figure 26 a). Twinning structures are very visible because of the shapes and orientations of the pits (Figure 26 b). The shapes of the etch pits appearing on the {110} planes and the {111} planes are of triangular forms. The shape of the etch pits appearing on the {100} planes is rectangular. Figure 26(c) and (d) show the

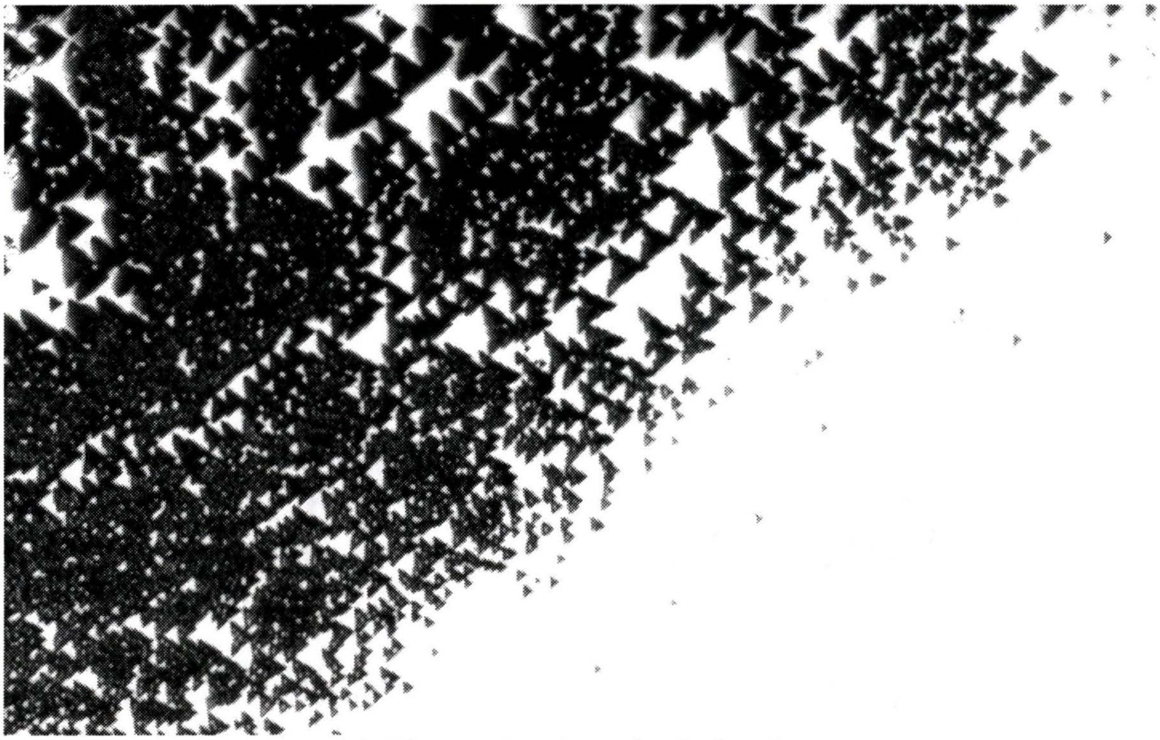

(a). Fluctuation in etch pit density.

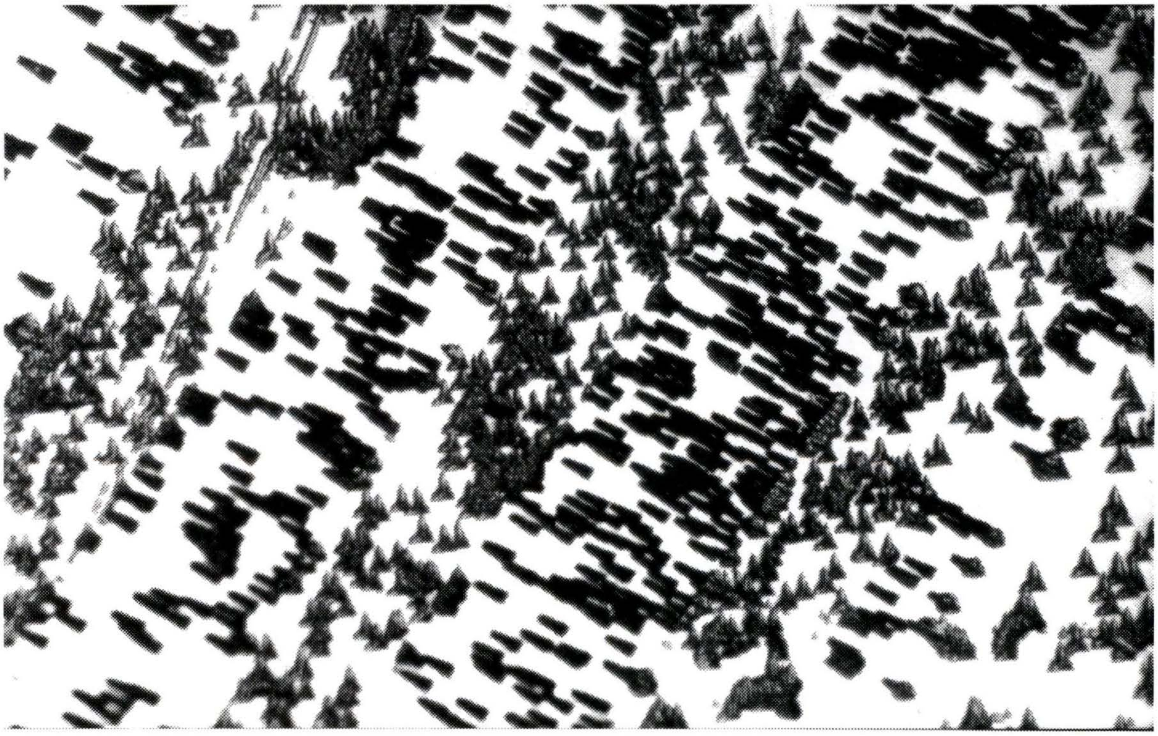

(b). Etch pits on twinning structures.

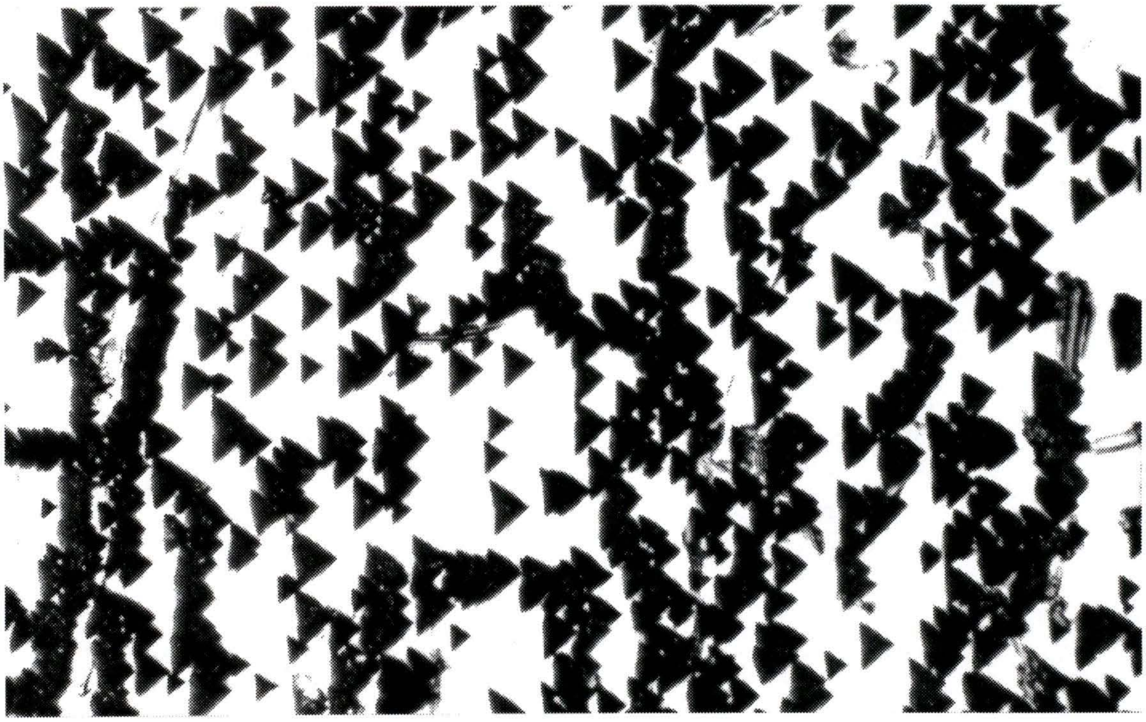

(c). Etch pits on the surface near-parallel {110} planes.

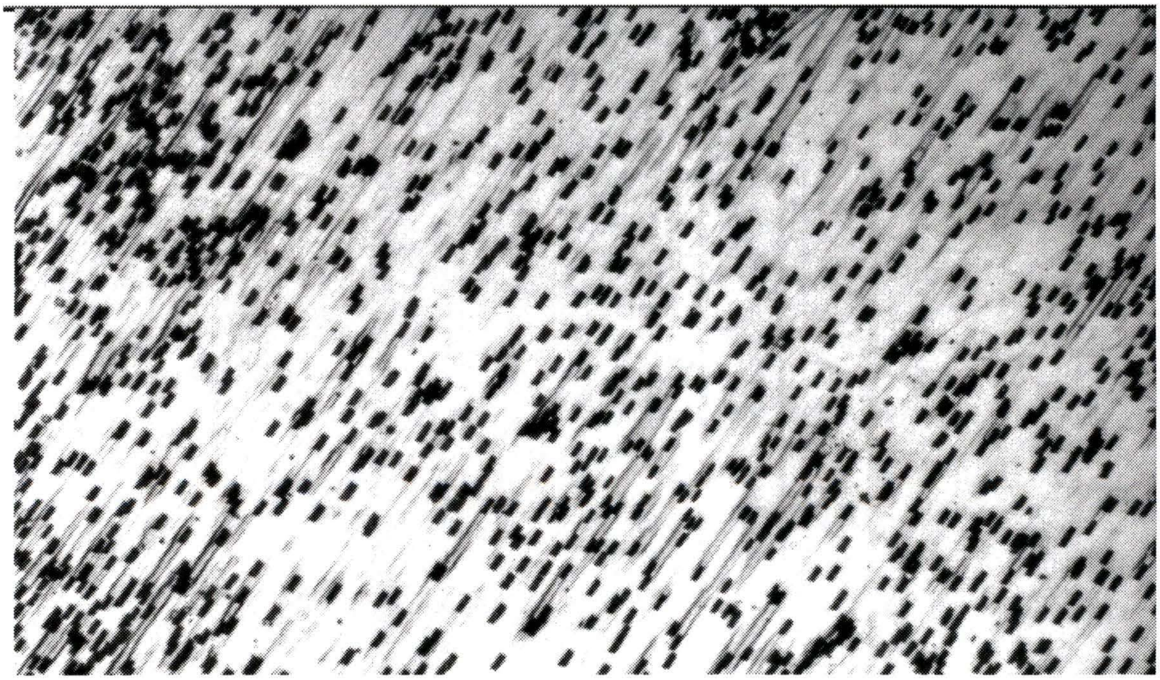

(d). Etch pits on the surface near-parallel {100} planes.

Figure 26. Etch pits on the wafer surfaces.

etch pits on the face near paralleling to the {110} planes and on the face near paralleling to the {100} planes. The average etch pit densities are between 10^4 ~10^5 cm^{-2}. This density is in the same range, compared with other authors' results of crystals grown from Bridgman and VGF techniques (T. Asahi, 1996).

5.3 Resistivities

The resistivities and hall mobilities of the CdTe/CdZnTe crystals are measured by the Van Der Pauw method (Van Der Pauw, 1958). Four Ohmic contacts (see Appendix 2) were formed by vacuum Au deposition on each wafer that was lapped and polished with mechanical and chemical methods. After deposited with Au, the samples were immediately put into the baking furnace and baked for 10 min at 500°C. During the baking, hydrogen was kept in flow through the furnace to protect the samples from oxidizing.

The results of Hall measurements are shown in Table 8. The range of resistivities is from $10^1\Omega \cdot \mathrm{cm}$ to $10^3\ \Omega \cdot \mathrm{cm}$ for un-doped CdTe and CdZnTe crystals. The resistivities obtained in our experiments are low compared with the results of other authors (see Table 9). The resistivities for un-doped CdTe/CdZnTe can reach to the order of $10^8\ \Omega \cdot \mathrm{cm}$. The explanation of such electrical properties obtained for our crystals is as follows.

Table 8. Electrical properties of the CdTe/CdZnTe crystals (300 K).

Ingot number	Ingot	Resistivity Ohm-cm	μ cm^2/V·Sec	Carr. Conc. Carr./cm^3	Cd reservoir Temperature (°C)
01	CdTe	3.61×10^1	8.38×10^3	2.06×10^{13}	785
02	$Cd_{0.96}Zn_{0.04}Te$	1.76×10^2	2.29×10^4	1.55×10^{12}	800
03	$Cd_{0.96}Zn_{0.04}Te$	9.42×10^2	5.23×10^4	1.27×10^{11}	825
05	$Cd_{0.96}Zn_{0.04}Te$	1.35×10^1	4.27×10^2	1.08×10^{15}	785
07	$Cd_{0.96}Zn_{0.04}Te$	2.54×10^1	3.50×10^3	7.01×10^{13}	785
08	$Cd_{0.9}Zn_{0.1}Te$	1.32×10^3	1.41×10^4	3.35×10^{11}	785

Table 9. Resistivity review of CdTe/CdZnTe crystals.

Method	Materials	Resistivities	Refs.
HPB	$Cd_{0.96}Zn_{0.04}Te$	$1.1 \times 10^{10}\ \Omega\cdot$cm	(Doty, 1992)
THM	CdTe doped with Cl	over $10^8\ \Omega\cdot$cm	(Ohmori, 1993)
VB	CdTe	$8.3 \times 10^3\ \Omega\cdot$cm	(Casagrande, 1993)
VGF	$Cd_{0.97}Zn_{0.03}Te$	30-37 $\Omega\cdot$cm	(Asahi, 1996)
HPB	CdZnTe with 0.04-0.2 Zn	$10^9\Omega\cdot$cm	(Chibani, 1996)
HPB	CdZnTe with 0.2-0.4 Zn	$10^9\ \Omega\cdot$cm	(Kolesnikov, 1997)

(1) The point defects of Cd vacancies and Te interstitials. The carrier concentration of undoped semiconducting crystals is dominated by native point defects. Therefore, the electrons or holes induced by these point defects contribute to the conductivity of the crystals. It is found that the composition of crystal grown under equilibrium conditions from a stoichiometric melt always consists of a small Te excess of about 10^{17} atoms per cm^3 (P. Rudolph, 1994). That means that some amount of Cd is released from the soichiometric liquid of CdTe during the growth. Cd vacancies on

the Te – rich side are formed. From Table 9, we can see that almost all the CdTe/CdZnTe crystals grown by the HPBM method exhibit high resistivities. The explanation is that no Cd is released from stoichiometric liquid of CdTe/CdZnTe using high pressure growth methods and the growth is a stoichiometric growth. Therefore, fewer Cd vacancies are created during crystal growth. That is why such large differences in electrical properties exist between crystals grown by HPBM and those grown by other methods. HPBM is originally selected to reduce the mean free path for vapor species and inhibit evaporation of the charge, and no one mentions the relations between high resistivity of the crystals and the high pressure method.

(2) Impurities in the crystals. The laboratory environment is not clean to industrial criteria and the crystals are contaminated by other chemicals such as Ga .

Chapter 6 Conclusions

For the purpose of growing large-size single crystals of CdTe/CdZnTe semiconductors, a combined experimental/theoretical study was undertaken. The results of this study were presented in this thesis.

In the theoretical part, special attention was paid to the discussion of the phenomena of superheating and supercooling. These phenomena play an important role in the formation processes of nucleation of the crystal. Superheating (<10 k) guaranties the growth of single crystals in the beginning, but limits the size of crystal grains. Superheating, however, to a certain extent can lead to the formation of polycrystalline nucleation in the beginning because of supercooling, but favors the formation of large-size single crystal grains during later stages of growth. These two phenomena are often coupled together under certain conditions. The understanding of these two phenomena has been used as an important guide for the experiments.

The development of the VGF crystal growth facility, temperature profiles based on the theoretical study and the synthesis and crystal growth experiments that were conducted constitute the major part of this thesis. The development of some special experimental techniques can be considered unique and original.

The VGF crystal growth apparatus was developed by modifying the existing LPEE crystal growth facility. The three zone furnace is successfully used for the VGF method. This makes the VGF apparatus simple and less expensive.

For melt growth in general, and the VGF growth in particular, the design of growth temperature profiles is one of the most important processes. In this design the phenomena of superheating and supercooling play a significant role. Unique temperature profiles were designed for experiments with different material compositions. The key points in the design are both the utilization of superheating and the confinement of supercooling. In the beginning, supercooling was avoided at the ampoule tip (by keeping this part under the superheating limit) in order to allow the formation of large-size single crystal grains initially. Then, the part above the tip section was kept at high superheating temperature to encourage the continuation of the growth of large-size single crystal grains. The results of our experiments verify that the design of the temperature profiles is successful.

Eight crystal growth experiments were conducted. A number of large single crystal grains of CdTe/CdZnTe were successfully grown. Large-size single crystal grains in the whole ingots were obtained in all experiments, although some of them were broken due to high stress. Therefore, the first part of the ingots is also useful. The successful growth of CdTe/CdZnTe crystals was the first step, and alone is a significant contribution to the field.

However, one should also determine the material properties of grown crystals to see whether they are of desired quality to meet the requirements of intended applications. In this direction, some properties of the grown crystals were measured.

One of the most important properties is the etch-pit density. The etch-pit density obtained from our samples is the same (or less) compared to those obtained by other researchers, showing that the defects in the single crystal grains are not high. The etch pit density, however, is not uniform. It is higher near the grain boundary than in the inner region of the grains. This implies that the stress in the crystals is higher near the grain boundary than inside. This also explains the cracks seen between single crystal grains. In some experiments this high stress broke the ampoules in the cooling processes following the growth.

The resistivity measurements were carried out using the Van der Pauw method. The measured resistivities of our crystals are much lower compared with those of materials obtained by other techniques. It is thought that the following might have contributed to such a result: the crystals were not grown in stoichiometry, and grown crystals were possibly contaminated during the growth process.

In conclusion, the three zone furnace is for the first time successfully used for the VGF method. The advantages of superheating in different extents are combined together to design unique temperature profiles. Large-size single crystals in whole ingots were obtained using these temperature profiles by controlling superheating and supercooling in the crystal growth process.

Future work should be focused on the improvement of resistivity of grown crystals, and the reduction of thermal stress in the grain boundary regions. To fully characterize the properties of grown crystals, further measurements are required.

Bibliography

1. T. Asahi, O. Oda, Y. Taniguchi and A. Koyama, "Growth and characterization of 100 mm diameter CdZnTe single crystals by the vertical gradient freezing method" *Journal of Crystal Growth*, **161**, 1996, p. 20.

2. T. Asahi, O. Oda, Y. Taniguchi and A. Koyama, "Characterization of 100 mm diameter CdZnTe single crystals grown by the vertical gradient freezing method", *Journal of Crystal Growth*, **149**, 1995, p. 23.

3. M. Azoulay, A. Raizman and G. Gafni, "Crystalline perfection of melt-grown CdTe", *Journal of Crystal Growth*, **101**, 1990, p. 256.

4. R. U. Barz, P. Sabhapathy and M. Salcudean, "A numerical study of convection during THM growth of CdTe with ACRT", *Journal of Crystal Growth*, **180**, 1997, p.566.

5. P. Brunet, A. Katty, D. Schenider, A. Tromson-Carli and R. Triboulet, "Horizontal Bridgman growth of large high quality $Cd_{1-y}Zn_yTe$ crystals", *Materials Science and Engineering*, **B16**, 1993, p. 44.

6. J. F. Butler, F. P. Doty, B. Apotovsky, J. Lajzerowicz and L. Verger, "Gamma – and X-ray detectors manufactured from Cd1-xZnxTe grown by a high pressure Bridgman method", *Materials Science and Engineeting*, **B16**, 1993, p. 291.

7. L. G. Casagrande, D. J. Larson, Jr., D. D. Marzio, J. Wu and M. Dudley, "The growth and comparison of large-diameter vertical Bridgman CdZnTe and CdTe", *Journal of Crystal Growth*, **137**, 1994, p. 195.

8. L. G. Casagrande, D. D. Marzio, M. B. Lee, D. J. Larson, Jr., M. Dudley and T. Fanning, "Vertical Bridgman growth and characterization of large-deameter single-crystal CdTe", *Journal of Crystal Growth*, **128**, 1993, p. 576.

9. P. Cheuvart, U. El-Hanani, D. Schneider and R. Triboulet, "CdTe and CdZnTe crystal growth by horizontal Bridgman technique", *Journal of Crystal Growth*, **101**, 1990, p. 270.

10. L. Chibani, M. Hage-Ali and P. Siffert, "Electrically active defects in detector-grade CdTe:Cl and CdZnTe materials grown by THM and HPBM", *Journal of Crystal Growth*, **161**, 1996, p. 153.

11. P. N. Cooper, Introduction to Nuclear Radiation Detectors, Cambridge University Press, 1986.

12. S. Dost, and Z. Qin, "A Model for Liquid Phase Electroepitaxy under an External Magnetic Field PART-I. Theory", *Journal of Crystal Growth*, **153**, 1995, p. 123.

13. S. Dost and Z. Qin, "A Model for Liquid Phase Electroepitaxial Growth of Ternary Alloy Semiconductors. PART I – Theory", *International Journal of Applied Electromagnetics and Mechanics*, **7**, 1996, p. 109.

14. S. Dost and J. Su, "A Linear Morphological Stability Analysis for the Solid-Liquid Interface in Liquid Phase Electroepitaxy of GaAs", *Journal of Crystal Growth*, **167**, 1996, p. 305.

15. F. P. Doty, J. F. Butler, J. F. Schetzina and K. A. Bowers, "Properties of CdZnTe crystals grown by a high pressure Bridgman method", *Journal of Vacuum Science and Technology*, **B10**, 1992, p.1418.

16. F.Dupret and N. van der Bogaert, Bulk Crystal Growth, Handbook of Crystal Growth 2, editor: D. T. J. Hurle, North-Holland, 1994.

17. G. Entine, P. Waer, T. Tiernan and M. R. Squillante, "Survey of CdTe nuclear detector applications", *Nuclear Instruments and Methods*, **A283**, 1989, p.282.

18. W. J. Everson, C. K. Ard, J. L. Sepich, B. E. Dean and G. T. Neugebauer, "Etch pit characterization of CdTe and CdZnTe substrates for use in mercury cadmium telluride epitaxy", *Journal of Electronic Materials*, **24**, 1995, p. 505.

19. M. M. Faktor and I. Garrett, Growth of Crystals from the Vapor, Halsted Press, a Division of John Wiley & Sons, Inc., New York, 1974.

20. J. Fraden, AIP Handbook of Modern Sensors Physics, Designs and Applications, American Institute of Physics, New York, 1993.

21. V. M. Glazov, Liquid Semiconductors, Plenum press, New York, 1969.

22. K. Grasza, U. Z. Grasza, A. Jedrzejczak, R. R. Galazka, J. Majewski, A. Szadkowski and E. Grodzicka, "A novel method of crystal growth by

physical vapour transport and its application to CdTe", *Journal of Crystal Growth*, **123**, 1992, p. 519.

23. I. Hahnert, M. Muhlberg, H. Berger and Ch. Genzel, "Study of the defect structure of CdTe-rich II-VI single crystals", *Journal of Crystal Growth*, **142**, 1994, p. 310.

24. R. Hultgren, F. R. Desai and A. Kelley, Selected Values of the Thermodynamic Properties of the Elements, Metals Park, Ohio: American Society for Metals, 1973.

25. M. Inoue, I. Teramoto and S. Takayanagi, "Etch pits and polarity in CdTe crystals", *Journal of Applied Physics*, **33**, 1962, p. 2578.

26. E. Kaldis and M. Piechotka, Bulk Crystal Growth, Handbook of Crystal Growth **2,** editor: D. T. J. Hurle, North-Holland, 1994.

27. H. W. King, X-ray analysis of Engineering Materials, Text Book, University of Victoria, 1997.

28. N. N. Kolesnikov, A. A. Kolchin, D. L. Alov, Yu. N. Ivanov, A. A. Chernov, M. Schieber, H. Hermon, R. B. James, M. S. Goorsky, H. Yoon, J. Toney, B,Brunett and T. E. Schlesinger, "Growth and characterization of p-type Cd1-xZnxTe (x = 0.2, 0.3, 0.4)", *Journal of Crystal Growth*, **174**, 1997, p. 256.

29. T. S. Lee, S. B. Lee and J. M. Kim, "Vertical Bridgman Techniques to Homogenize Zinc Composition of CdZnTe Substrates", *Journal of Electronic Materials*, **24**, 1995, p. 1057.

30. E. Monberg, Bulk Crystal Growth, Handbook of Crystal Growth **2,** editor: D. T. J. Hurle, North-Holland, 1994.

31. K. Nakagawa, K. Maeda and S. Takeuchi, "Observation of dislocations in cadmium telluride by cathodoluminescence microscopy" *Applied Physics Letters*, 34, 1979, p. 574.

32. O. Oda, K. Hirata, K. Imura and F. Tsujino, "Large diameter CdTe single crystals – crystal growth and the evaluation", *Japanese Society of Apply Physics*, **55**, 1986, p. 1084.

33. M. Ohmori and Y. Iwase, "High quality CdTe and its application to radiation detectors", *Materials Science and Engineering*, **B16**, 1993, p. 283.

34. W. Palosz, F. R. Szofran and S. L. Lehoczky, "Experimental studies on mass transport of cadmium-zinc telluride by physical vapor transport", *Journal of Crystal Growth*, **148**, 1995, p. 56.

35. L.J. van der Pauw, "A method of measuring specific resistivity and Hall effect of discs of arbitrary shape", *Philips Research Reports*, **13**, 1958, p. 174.

36. S. B. Qadri, E. F. Skelton, A. W. Webb and J. Kennedy, "Evidence for bond strengthening in $Cd_{1-x}Zn_xTe$ ($x = 0.04$)", *Applied Physics Letters*, **46**, 1985, p. 257.

37. P. Rudolph, A. Engel, I. Achentke and A. Grochocki, "Distribution and genesis of inclusions in CdTe and (Cd, Zn) Te single crystals grown by the Bridgman method and by the travelling heater method", *Journal of Crystal Growth*, **147**, 1995, p. 297.

38. P. Rudolph, "Fundamental studies on Bridgman growth of CdTe", *Progress in Crystal Growth and Characterization*, **29**, 1994, p. 275.

39. P. Rudolph and M. Muhlberg, "Basic problems of vertical Bridgman growth of CdTe", *Materials Science and Engineering*, **B16**, 1993, p. 8.

40. P. Rudolph, M. Neubert and M. Muhlberg, "Defects in CdTe Bridgman monocrystals caused by nonstoichiometric growth conditions", *Journal of Crystal Growth*, **128**, 1993, p. 582.

41. M. Schenk, I. Hahnert, L. T. H. Duong and H.-H. Niebsch, "Validity of the lattice-parameter Vegard-rule in $Cd_{1-x}Zn_xTe$ solid solutions", *Crystal Research and Technology*, **31**, 1996, p. 665.

42. M. Schieber, C. Ortale, L. Van Den Berg, W. Schnepple, L. Keller, C.N.J. Wagner, W. Yelon, F. Ross, G. Georgeson and F. Milstein, "Correlation between mercuric iodide detector performance and crystalline perfection", *Nuclear Instruments and Methods in Physics Research*, **A283**, 1989, p. 172.

43. J. P. Schwartz, T. Tung and R. F. Brebrick, "Partial pressures over HgTe – CdTe solid solutions I. Calibration experiments and results for 41.6 mole percent CdTe", *Journal of the Electrochemical Society*, **128**, 1981, p. 438

44. J. Shen, D. K. Aidun, L. Regel and W. R. Wilcox, "Characterization of precipitates in CdTe and Cd1-xZnxTe grown by vertical Bridgman-Stockbarger technique", *Journal of Crystal Growth*, **132**, 1993, p. 250.

45. R. Shetty, R. Balasubramanian and W. R. Wilcox, "Surface tension and contact angle of molten semiconductor compounds I. Cadmium telluride", *Journal of Crystal Growth*, **100**, 1990, p. 51.

46. J. Steininger, A. J. Strauss and R. F. Brebrick, "Phase diagram of the Zn-Cd-Te ternary system", *Journal of Electrochemical Society: Solid state science*, **117**, 1970, p. 1305.

47. Y. Tao and S. Kou, "Segregation reduction in vertical Bridgman crystal growth of CdZnTe", *Journal of Crystal Growth*, **181**, 1997, p. 301.

48. R. Triboulet and Y. Marfaing, "CdTe growth by multipass THM and sublimation THM", *Journal of Crystal Growth*, **51**, 1981, p. 89.

49. M.S. Tyagi, Introduction to Semiconductor Materials and Devices, John Wiley & Sons, 1991.

50. N. Yellin and S. Szapiro, "Calculation of the partial vapor pressures of tellurium and cadmium over non-stoichiometric CdTe in the temperature range 750-1050°C", *Journal of Crystal Growth*, **73**, 1985, p.77.

Appendix 1 X-ray Interaction with Matter

There are three interesting interaction mechanisms for radiation measurements when x-ray or γ-ray is incident on materials: photoelectric absorption, Compton scattering and pair production.

1. Photoelectric absorption

In this interaction the x-ray quanta interact with strongly bound electrons in the innermost or *K*-shells of the absorber atoms. The x-ray quanta disappear completely and produce fast electrons and in turn these electrons cause ionization in a similar manner. The photoelectric effect is stronger for absorber materials of high atomic number and the probability of the photoelectric interaction occurring is roughly proportional to Z^n/E^3 (P. N. Cooper, 1986), where n is between 4 and 5 and E is the energy of the x-ray or γ-ray quantum. For this reason high atomic number materials are better for shielding and detection purposes of x-rays and γ-rays.

2. Compton scattering

Compton scattering is an interaction between an x-ray or γ-ray and free or only weakly bound electrons. Only part of quantum energy is transferred to the electron and is scattered at a lower energy in the process. The energy of the scattered quantum is a function of the angle of scatter. The Compton scattering energy is always less than the incident energy. The probability of Compton scattering depends upon the number of available electrons as well as on the cross-section, and it increases with the atomic number of the scattering materials and the incident quantum energy.

3. Pair production

This interaction results in the production of a positron and an electron if the incident energy exceeds twice the rest mass energy equivalent of the electron or 1.022 MeV. The incident quantum disappears completely and an electron-positron pair is created. The rest energy, (E –1.022 MeV), is shared by the positron and the electron. Therefore, pair production can only occur when the incident energy is twice or more than twice the rest energy of electron mass.

Among these three effects, photoelectric effect is the main process and the most useful effect that x-ray or γ-ray energy deposits in the crystal. The photoelectric interaction produces a quantity of electrons (a quantity of light for scintillating materials) proportional to the incident energy. Other effects interacted with materials can be seen in Figure 27 (Cooper, 1986), which shows result produced by 1 MeV γ-rays incident on a sodium iodide detector. The full energy peak or photopeak is the result of photoelectric effect. The lower pulse height continuous distribution results from the electrons produced in Compton scatters. The further low pulse height peak results from γ-rays that have been scattered by Compton effect at the angle of around 180° from the source holder or surrounding shielding. The Full Width at Half Maximum (FWHM) of the full energy peak is exploited to describe the quality (the resolution) of detectors. The narrower the FWHM, the higher the resolution of the detector.

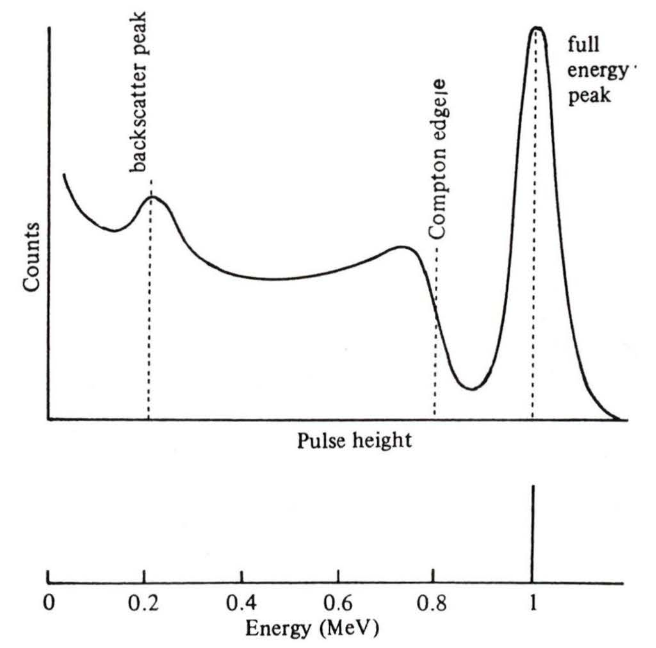

Figure 27. Typical pulse height spectrum produced by 1 MeV γ-rays incident on a sodium iodide detector (Cooper, 1986).

Appendix 2 Physics of Semiconductors

Some important characteristics of semiconductors, which are mentioned in this thesis, are reviewed briefly in this section.

Free carrier concentration

One of the most important characteristics of a semiconductor is its carrier concentration. Ideally, a pure crystal semiconductor contains no impurities and no lattice defects. Such semiconductors have as many vacant sites as the number of free electrons, and they are called intrinsic semiconductors, and the hole and electron pairs are called intrinsic charge carriers. How are the electron-hole pairs created? For intrinsic semiconductors, the thermal vibrations of lattice atoms exist, which results in excitation of some electrons in the valence band to the conduction band, leaving an equal number of holes in the valence band. This process of pair generation is called the thermal generation process. The total number of holes and electrons in a piece of semiconductor is rarely of any interest. What is important is the number of carriers per unit volume, known as the carrier density or carrier concentration, and it is expressed as the number of carriers per cm^3. For intrinsic semiconductors, $p = n = n_i$, that means that the holes density (p) is equal to the electron density (n). The subscript i is used to denote the intrinsic of semiconductors. The intrinsic concentration varies with the temperature and reaches a steady state in equilibrium.

In practice, almost all semiconductors are doped, intentionally or not, to form n- or p-type materials. Therefore, charge carriers can be created by introducing small quantities of the proper chemical impurity atoms. For n-type semiconductor materials, the impurity atom added takes in the crystal lattice the position of the original atom and contributes an electron to the conduction band without creating any holes in the valence band. Those substitutional impurity atoms are called donors. The majority carriers in n-type semiconductors are electrons, and the Fermi level is nearer the conduction band. For p-type semiconductor materials, the impurity atom contributes a hole in the valence band without creating an electron in the conduction band. Those impurity atoms in p-type materials are called acceptors. The majority carriers are holes, and the Fermi level is nearer the valence band.

Drift current and mobility

Every semiconductor contains free carriers and these carriers (electrons and holes) are in random motion because of their thermal energy. When a low electric field is applied to a crystal, the electrons and holes have two kinds of motion: the thermal random motion and the motion by the electric field. In total, the free carriers have a movement in the direction of the electric field. This motion is known as the drift motion. The current created by the carrier drift is called the drift current. Thus, it is clear that in the presence of an electric field, an electron acquires a drift velocity. The resultant velocity is the vector sum of the drift velocity and the random thermal velocity. The drift velocity v_d is proportional to the electric field strength ε, and the proportionality constant is defined as the mobility μ in cm^2/V. Sec., $v_d = \mu\varepsilon$. For non-cryogenic temperature, the mobility decreases while the temperature and impurity concentration increase. Also, as the mass of carrier increases, the mobility decreases; thus, for a given impurity concentration and temperature the electron mobility is larger than the hole mobility.

Resistivity and Hall effect

The resistivity ρ is defined as the proportionality constant between the electric field and the current density, $\varepsilon = \rho \mathbf{J}$. The reciprocal value of the resistivity is the conductivity, σ, and $\mathbf{J} = \sigma\varepsilon$. For semiconductors with both electrons and holes as free carriers, the resistivity is

$$\rho = 1/\sigma = 1/[q(\mu_n + \mu_p)]$$

in n-type semiconductors

$$\rho \approx 1/q\mu_n n$$

and, in p-type semiconductors

$$\rho \approx 1/q\mu_p p$$

In semiconductors, the resistivity can range between wide limits. M.S. Tyagi (Tyagi, 1991) reports that this range is from 10^{-3} to 10^{8} $\Omega\cdot$cm; this classification is quite arbitrary. Materials whose resistivities are over 10^{8} $\Omega\cdot$cm are also considered semiconductors. When semiconductors are intrinsic, the resistivities reach a maximum. The resistivities of intrinsic GaAs and CdTe are ~ 10^{8} $\Omega\cdot$cm and over 10^{8} $\Omega\cdot$cm. The resistivity drops rapidly with the increase of impurity levels.

To measure the carrier concentration and sign directly, the most common method relies on the Hall effect. Consider a rectangular sample of a uniformly doped, p-type semiconductor and put it into an electric field (x direction) and a magnetic field (y direction). The holes in the semiconductor are subjected to two kinds of forces. One is the magnetic force, which is called the Lorenz force and acts in the negative z-direction. This force causes holes to be accumulated on the bottom surface of the semiconductor, which in turn gives rise to another electric field (Hall field) and its direction is along the z-axis. This electric field exerts a force along the z-axis direction. When these two forces are equal, there is no net current along the z-direction. The Hall field can be measured externally and is given by

$$\varepsilon_z = R_H J_x B_y$$

where R_H is the Hall coefficient and is given by

$$R_H = 1/qp_0$$

where p_0 is the equilibrium concentration of holes in the sample. A similar analysis can be carried out for an n-type semiconductor, and the Hall coefficient is given by

$$R_H = - 1/qn_0$$

where n_0 is the equilibrium concentration of electrons in the sample.

Ohmic contacts

The measurement of semiconductor characteristics requires ohmic contacts to which connections can be made. An ohmic contact is a metal-semiconductor contact whose resistance is negligibly small compared with the resistance of the semiconductor specimen to which the contact is applied. The ohmic contact serves as a means of taking current in and out of the device.

When a metal comes into contact with a semiconductor, a Schottky barrier will form because of the different work functions of the metal and the semiconductor. If the barrier height is small compared with kT (k is the Boltzman's constant and T is the temperature in Kelvin), a low resistance contact is obtained. Carriers can flow over the barrier in either direction without any impediment. In principle, such contacts can be made by using a metal with a work function less than the work function of an n-type semiconductor or greater than the work function of a p-type semiconductor. However, there are very few metal-semiconductor combinations that satisfy this condition. The majority of ohmic contacts involve a thin layer of very heavily doped semiconductor immediately adjacent to the metal, so that the depletion layer is so thin that the carriers can readily tunnel through it.

Appendix 3 Material impurities

The single elements that were used for synthesis of CdZnTe are cadmium, zinc and tellurium. The level of impurity was provided by the manufacturer, Noranda Advanced Materials. In the following tables, the impurities of these elements are presented.

Table 10. Cadmium Impurities.

Element	Impurity (ppb)	Element	Impurity (ppb)
Li	<0.8	Br	<10
Be	<0.3	Rb	<0.2
B	<0.5	Sr	<0.1
C	900	Y	<0.1
N	150	Zr	<0.07
O	1000	Nb	<0.1
F	<50	Mo	<0.3
Na	2	Pd	
Mg	<0.3	Ag	<20
Al	<0.2	Cd	Matrix
Si	<0.8	In	<90
P	<0.4	Sn	<4
S	<0.5	Sb	<0.2
Cl	6	Te	<4
K	<5	I	<10
Ca	<4	Cs	<0.2
Sc	<0.3	Ba	<1
Ti	<0.06	La	<4
V	<0.1	Ce	<5
Cr	<0.3	Hf	<0.07
Mn	<25	Ta	
Fe	<20	W	<0.1
Co	<0.07	Pt	3
Ni	<0.4	Au	<10
Cu	<0.4	Hg	<0.3
Zn	30	Ti	<0.1
Ga	<0.4	Pb	<0.1
Ge	<0.6	Bi	<0.1
As	<10	Th	<1
Se	<5	U	<0.04

Table 11. Zinc Impurities.

Element	Impurity (ppb)	Element	Impurity (ppb)
Li	<0.5	Br	<10
Be	<0.2	Rb	<0.1
B	10	Sr	<0.1
C	730	Y	<0.08
N	400	Zr	<0.05
O	1500	Nb	<0.2
F	<100	Mo	<0.2
Na	<0.3	Pd	
Mg	<0.2	Ag	<1
Al	<0.1	Cd	20
Si	<2	In	<0.1
P	<0.2	Sn	<0.5
S	<50	Sb	<0.1
Cl	<3	Te	<2
K	<70	I	<0.8
Ca	<2	Cs	<30
Sc	<0.06	Ba	<5
Ti	<0.06	La	<0.04
V	<0.09	Ce	<0.1
Cr	<2	Hf	<0.05
Mn	<0.3	Ta	
Fe	80	W	<0.3
Co	<0.05	Pt	<0.1
Ni	0.6	Au	<5
Cu	<80	Hg	<0.3
Zn	Major	Ti	<0.1
Ga	<5	Pb	<0.09
Ge	<1	Bi	<0.07
As	<0.1	Th	<0.03
Se	<5	U	<0.03

Table 12. Tellurium Impurities.

Element	Impurity (ppb)	Element	Impurity (ppb)
Li	<3	Br	
Be	<1	Rb	<0.7
B	<2	Sr	<0.5
C	1000	Y	<0.4
N	500	Zr	<0.2
O	1400	Nb	<0.3
F	<40	Mo	<0.5
Na	7	Pd	
Mg	<2	Ag	<1
Al	<0.7	Cd	<3
Si	20	In	<0.4
P	<1	Sn	<2
S	<3	Sb	<50
Cl	0.9	Te	Matrix
K	<25	I	<600
Ca	<20	Cs	<3
Sc	<0.3	Ba	<3
Ti	<0.2	La	<0.5
V	<0.1	Ce	<5
Cr	<1	Hf	<0.3
Mn	<0.6	Ta	
Fe	<0.4	W	<0.4
Co	<0.3	Pt	<0.9
Ni	<0.6	Au	<10
Cu	<2	Hg	<1
Zn	<3	Ti	<0.6
Ga	<1	Pb	<0.6
Ge	<3	Bi	<0.4
As	<2	Th	<0.1
Se	40	U	<0.1

VITA

Surname: Li Given Name: Lingzhi

Place of Birth: Jixi, Heilongjiang, China

Educational Institutions Attended:

University of Victoria	1996 to 1999
Harbin Institute of Technology	1985 to 1988
Harbin University of Science and Technology	1979 to 1983

Degrees Awarded:

M.Sc	Harbin Institute of Technology	1988
B.Sc.	Harbin University of Science and Technology	1983

Publications:

1. Lingzhi Li and Sadik Dost, Growth of CdTe/CdZnTe Single Crystals by the Vertical Gradient Freezing Method, May 30 – June 3, 1999, Hamilton, Ontario, Canada.
2. Fengmei Liu, Lingzhi Li and Chi Zhou et al, Design and comparative performances of two kinds of transversely excited CO_2 laser Coherent Laser Radar, July 23-27, 1995, Keystone, Colorado, USA.
3. Lingzhi Li, Qingchun Hou and Zhu Yuet al, Measurement of light scattering of human red blood cells, J. Harbin University of Science and Technology, Vol.19, No.4, 72, 1995.
4. Lingzhi Li and Tailong Gui, A mini-CO_2 laser without water-cooling system, J. Harbin University of Science and Technology, Vol.18, No.2, 66, 1994.

PARTIAL COPYRIGHT LICENSE

Title of Thesis:

Growth of CdTe/CdZnTe Single Crystals by the Vertical Gradient Freezing Method

Author [redacted]

Lingzhi Li
March 1, 1999